INL/EXT-12-27668

Advanced Fuels Campaign 2012 Accomplishments

November 2012

The INL is a U.S. Department of Energy National Laboratory
operated by Battelle Energy Alliance

INL/EXT-12-27668
FCRD-FUEL-2013-000032

Advanced Fuels Campaign
2012 Accomplishments

November 2012

Idaho National Laboratory
Advanced Fuels Campaign
Idaho Falls, Idaho 83415

http://www.inl.gov

Prepared for the
U.S. Department of Energy
Office of Nuclear Energy
Under DOE Idaho Operations Office
Contract DE-AC07-05ID14517

INL/EXT-12-27668

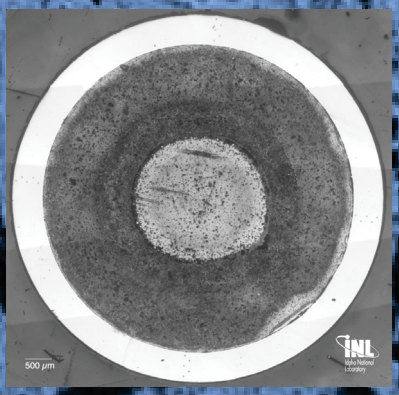

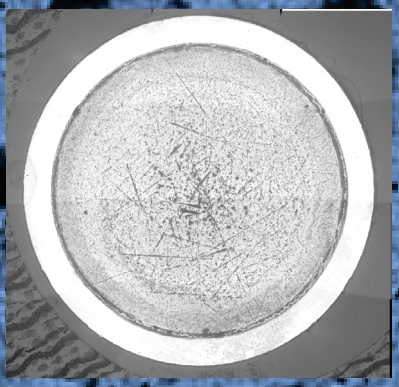

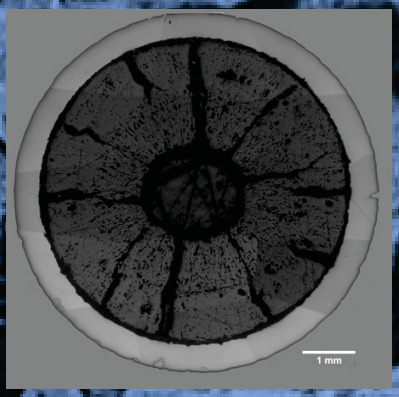

Advanced Fuels Campaign
2012 Accomplishments

Prepared for
U.S. Department of Energy

Advanced Fuels Campaign

Revision 0
November 2012
FCRD-FUEL-2013-000032

FUEL CYCLE RESEARCH AND DEVELOPMENT

ADVANCED FUELS CAMPAIGN
FY 2012 ACCOMPLISHMENTS REPORT

INL/EXT-12-27668
FCRD-FUEL-2013-000032
Revision 0

November 2012

Compiled and edited by:

Lori Braase (lori.braase@inl.gov)
Douglas Hamelin (douglas.hamelin@inl.gov)
INL Systems Engineering

Approved by:

Jon Carmack
FCRD AFC National Technical Director

November 28, 2012
Date

EXECUTIVE SUMMARY

The Advanced Fuels Campaign (AFC) under the Fuel Cycle Research and Development (FCRD) program is responsible for developing fuels technologies to support the various fuel cycle options defined in the *DOE Nuclear Energy Research and Development Roadmap, Report to Congress, April 2010*. The fiscal year 2012 (FY 2012) accomplishments are highlighted below.

The Advanced Fuels Campaign (AFC) has the responsibility to develop advanced nuclear fuel technologies for the Department of Energy (DOE) Fuel Cycle Research and Development (FCRD) Program. AFC uses a "goal-oriented science-based approach" aimed at a fundamental understanding of the fuel fabrication methods and fuel and cladding performance under irradiation, enabling the pursuit of multiple fuel forms for the future fuel cycle options. This approach includes fundamental experiments, theory, and advanced modeling and simulation. The modeling and simulation activities for fuel performance are carried out under the Nuclear Energy Advanced Modeling and Simulation (NEAMS) program, which is closely coordinated with AFC.

In FY-2012, the scope was modified to include research and development of light water reactor (LWR) fuels with enhanced accident tolerance in addition to the long-term goal to develop transmutation fuel systems. The major areas of research for this new scope include enhancing the accident tolerance of fuels and materials, improving the fuel system's ability to achieve significantly higher fuel and plant performance, and developing innovations that provide major increases in burn-up and performance. The goal is advanced nuclear fuels and materials technologies that are robust, have high performance capability, and are more tolerant to accident conditions than traditional fuel systems. In this report the word "fuel" is used generically to include fuels, targets, and their associated cladding materials.

AFC management and integration activities included continued support for international collaborations, primarily with France, Japan, European Union, Republic of Korea, and China, as well as various working group and expert group activities in the Organization for Economic Cooperation and Development Nuclear Energy Agency (OECD NEA) and the International Atomic Energy Agency (IAEA). Three innovative fuel concepts were funded and managed under the respective technical areas. Quarterly campaign meetings focused on technical progress and incorporation of Light Water Reactor (LWR) fuel development in response to the Fukushima accident.

Technical highlights are reported under the following research and development (R&D) areas:

- Metallic-based Fuels Technologies, J. R. Kennedy, INL, Technical Lead
- Ceramic-based Fuels Technologies, K. McClellan, LANL, Technical Lead
- Microencapsulated Fuels Technologies, L. L. Snead, ORNL, Technical Lead
- Core Materials Technologies, S. Maloy, LANL, Technical Lead
- Irradiation Testing Technologies, S. L. Hayes, INL, Technical Lead
- Analytic Support, C. Unal, LANL, Technical Lead

Metallic-Based Fuels Technologies

Metallic-based Fuels Technologies focused on research and development to gain a fundamental understanding of metallic fuels. Priority was on low-loss fabrication methods and capability and on developing a fundamental understanding of the phase, microstructure, and chemical migration behavior of metallic fuel constituents. The desired outcome is to develop an understanding of the key phenomena affecting metallic fuel performance and behavior under irradiation.

Metallic-Based Fuels Technologies major accomplishments include:

- Completed the design of the remote fabrication capability.
- Installed a low loss casting furnace in inert atmosphere.

Ceramic-Based Fuels Technologies

Ceramic-based Fuels Technologies focused on the fundamental understanding of oxide fuels. Key challenges include the development of reliable, low-loss fuel fabrication methods and fuel technology development to enable major increases in fuel burn up and performance (reliability, power and safety) beyond current technologies. Activities fell within the following R&D categories: Ceramic process modeling (sintering); U-based fuel design, development and testing (International); mixed oxide (MOX) fuel processing and properties (International); and Technique development and reference materials.

Ceramic-Based Fuels Technologies major accomplishments include:

- Successful growth of thick film UO2 with embedded Xe.
- Construction and testing of a high temperature melting point apparatus.

Microencapsulated Fuels Technologies and Severe Accident Test Station

Microencapsulated Fuels Technologies focused on the application of coated particle fuel technology for advanced reactor platforms including LWR applications. It is highly integrated with direct modeling, fuel fabrication, irradiation testing, and post irradiation performance evaluation. FY 2012 focus areas included modeling, transuranic TRISO fuel, LWR microencapsulated fuel, and testing advanced clad and fuel materials for enhanced safety.

Microencapsulated Fuels Technologies major accomplishments include:

- Design and construction of a severe accident test station.
- Irradiation and PIE of surrogate FCM matrix.

Core Materials Technologies

Core Materials Technologies focused on fast reactor cladding materials for high dose applications and advanced LWR cladding for enhanced accident tolerance in knowledge base development for High Dose (up to 200 dpa), Core Materials Irradiation Data (ACO-3 duct testing and Fast Flux Test Facility [FFTF] Materials Open Test Assembly [MOTA] testing), and Advanced Material Development (advanced cladding materials and coatings/liners to mitigate fuel-cladding-chemical interaction [FCCI]).

Core Materials Technologies major accomplishments include:

- Completed tensile testing of high dose ODS and F/M steels.
- Demonstrated the effectiveness of a thin layer TiN coating on suppressing FCCI.

Irradiation Testing Technologies

Irradiation Testing Technologies focused on continued irradiation of fast reactor fuel concepts in Advanced Test Reactor (ATR), preparations for separate effects tests (SET) for fuel using the hydraulic rabbit facility in the High-Flux Isotope Reactor (HFIR), and postirradiation examinations (PIE) of fuels irradiated in ATR, Experimental Breeder Reactor II (EBR-II), and FFTF.

Irradiation Testing Technologies major accomplishments include:

- Completed irradiation of two transmutation fuel experiments.
- Completed baseline PIE of FFTF high burnup oxide and metallic fuels.

Analytic Support

Analytic Support is focused on the analysis of the impact of novel fuel forms on reactor operations and the development of fuel fabrication models, such as sintering, casting, etc. In addition, this is the primary interface with NEAMS to identify fuels and materials data needs.

Analytic Support major accomplishments include:

- Demonstrated the use of BISON fuel performance code for metallic fuel designs.
- Developed master sintering curves (MSC) for different O/M ratios for commercial feedstocks.

Innovative Transmutation Fuels Concepts

As part of FCRD's longer-term, science based focus, there is a desire to promote the generation of new ideas and foster exploration of transformational technology options. Three innovative transmutation fuels concepts were funded in FY 2011and continued work in FY 2012 focused on the following R&D areas:

- ***Advanced Metallic Fuel Concept for Reliable Performance to Ultra-High Burnup.*** As an outcome of the AFC call for innovative fuels concepts, Argonne National Laboratory (ANL) and Idaho National Laboratory (INL) received funding to begin developing an innovative design concept for ultra-high burnup sodium-cooled fast-reactor metallic fuel.
- ***Uranium Alloy Metal Fuel for Light Water Reactors.*** This project is developing a new, high density, uranium alloy metal fuel for LWRs. This fuel has the potential for increasing the linear heat rate and power density in a reactor while possibly providing more favorable reactivity temperature coefficients. More favorable reactivity temperature coefficients have the potential to improve transient maneuvering between power levels. In addition, it has the ability to establish better performance under accident conditions.
- ***The Vented Fuel Pellet/Getter Concept for High Burnup Fuel.*** This Brookhaven National Laboratory (BNL) concept is to extend the burnup of nuclear fuel by enhancing the release, transport, and sequestering of fission product gases from the fuel pellet to a plenum region in the fuel rod.

Intentionally left Blank

CONTENTS

FIGURES

TABLES

ACRONYMS

µ-XRD	Micro-focus X-ray Diffractometer
AFC	Advanced Fuels Campaign
ANL	Argonne National Laboratory
APT	Atom Probe Tomography
ASU	Arizona State University
ATF	Accident Tolerant Fuel
ATR	Advanced Test Reactor
BNL	Brookhaven National Laboratory
BSC	Bench Scale Casting
BSE	Backscattered Electron
CEA	Atomic Energy Commission (France)
CEFR	China Experimental Fast Reactor
CIAE	China Institute of Atomic Energy
CRADA	Cooperative Research and Development Agreement
CRIEPI	Central Research Institute of Electric Power Industry (Japan)
DFEM	Densification-Based Finite-Element Model
DOE	Department of Energy
dpa	Displacements Per Atom
DSC	Differential Scanning Calorimetry
DTG	Differential Thermogravimetry
DU	Depleted Uranium
EBR	Experimental Breeder Reactor
EBS	Ethylene Bis Stearamide
EBSD	Electron Backscatter Diffraction
EDM	Electron Discharge Machining
EFPD	Effective Full-Power Day
EPMA	Electron Probe Micro-Analyzer
FCCI	Fuel-Cladding-Chemical Interaction
FCM	Fully Ceramic Microencapsulated
FCMI	Fuel-Clad-Mechanical Interaction
FCRD	Fuel Cycle Research and Development
FE	Finite Element

FP	Fission Product
FFTF	Fast Flux Test Facility
FIB	Focused Ion Beam
FMEF	Fuels and Materials Examination Facility
FOA	Funding Opportunity Announcement
FY	Fiscal Year
GACID	Global Actinide Cycle International Demonstration
GB	Grain Boundary
Gen-IV	Generation IV
GFR	Gas-Cooled Fast Reactor
GTAW	Gas-Tungsten-Arc Welding
HFEF	Hot Fuel Examination Facility
HFIR	High-Flux Isotope Reactor
IAEA	International Atomic Energy Agency
IBAD	Ion Beam Assisted Deposition
IFR	Integral Fast Reactor
INERI	International Nuclear Energy Research Initiative
INL	Idaho National Laboratory
IRP	Integrated Research Proposal
IRT	Integrated Recycle Test
ITU	Institute for Transuranium Elements
JAEA	Japan Atomic Energy Agency
JFCS	Joint Fuel Cycle Studies
KAERI	Korean Atomic Energy Research Institute
LANL	Los Alamos National Laboratory
LEAP	Local Electrode Atom Probe
LED	Light-Emitting Diode
LHGR	Linear Heat Generation Rate
LLNL	Lawrence Livermore National Laboratory
LOCA	Loss of Coolant Accident
LRUS	Laser Resonance Ultrasonic Spectroscopy
LWR	Light Water Reactor
LWRS	Light Water Reactor Sustainability Program
MA	Minor Actinide

MAX	$M_{n+1} AX_n$ (Class of layered machinable ceramics)
MBM	MOOSE-BISON-MARMOT
MD	Molecular Dynamics'
MDD	Modified Direct Denitration
MOTA	Materials Open Test Assembly
MOX	Mixed Oxide
MPM	Mechanical Properties Microscope
MS	Mass Spectrometer
MSC	Master Sintering Curve
MXRD	Micro-focus X-ray Diffractometer
NE	Office of Nuclear Energy
NEAMS	Nuclear Energy Advanced Modeling and Simulation
NEUP	Nuclear Energy University Program
NFA	Nano-Strengthened Ferritic Alloy
NRC	Nuclear Regulatory Commission
O/M	Oxygen-To-Metal
ODS	Oxide Dispersion Strengthened
OECD-NEA	Organization for Economic Cooperation and Development-Nuclear Energy Agency
ORNL	Oak Ridge National Laboratory
PIE	Postirradiation Examination
PNNL	Pacific Northwest National Laboratory
PWR	Pressurized Water Reactor
R&D	Research and Development
RD&D	Research, Development, and Demonstration
RE	Rare Earth
RIAR	Research Institute of Atomic Reactors (Russia)
SATS	Severe Accident Test Station
SD	Smeared Density
SEM	Scanning Electron Microscope
SET	Separate Effects Test
SFR	Sodium Fast Reactor
SRNL	Savannah River National Laboratory
STA	Simultaneous Thermal Analyzer
STDM	Scanning Thermal Diffusivity Microscope

STEM	Scanning Transmission Electron Microscopy
TAC	Thermoacoustic
TCM	Thermal Conductivity Microscope
TG	Thermogravimetry
TIMS	Thermal Ionization Mass Spectrometer
TMS	The Minerals, Metal, and Materials Society
TMT	Thermo-Mechanical Treatments
TPM	Thermal Property Microscope
TRISO	Tristructural Isotropic
TRU	Transuranic
TSR	Technical Safety Requirements
IASCC	Irradiation Assisted Stress Corrosion Cracking
UCB	University of California-Berkeley
UCSB	University of California Santa Barbara
UHBR	Ultra-High Burnup Reactor
UHP	Ultra-High Burnup
ULT	Ultimate Tensile Strength
UTK	University of Tennessee Knoxville
WBS	Work Breakdown Structure
XRD	X-Ray Diffraction
YSZ	Yttria-Stabilized Zirconia

ADVANCED FUELS CAMPAIGN FY 2012 ACCOMPLISHMENTS REPORT

1. INTRODUCTION

One of the major research and development (R&D) areas under the Fuel Cycle Research and Development (FCRD) program is advanced fuels development. The Advanced Fuels Campaign (AFC) has the responsibility to develop advanced fuel technologies for the Department of Energy (DOE) using a science-based approach focusing on developing a microstructural understanding of nuclear fuels and materials.

Accomplishments made during fiscal year (FY) 2012 are highlighted in this report, which focuses on completed work and results. The process details leading up to the results are not included; however, the technical contact is provided for each section. The order of the accomplishments in this report is consistent with the AFC work breakdown structure (WBS).

2. CAMPAIGN MANAGEMENT AND INTEGRATION

J. Carmack, jon.carmack@inl.gov, INL

One of the most challenging aspects of the AFC is the management, integration, and coordination of the major R&D activities across multiple national laboratories and universities working to achieve this goal. Several management activities were accomplished in FY 2012 that supports the overall goals of the FCRD program. AFC interfaces and collaborates with the FCRD campaigns, industry, various DOE programs and laboratories, federal agencies (e.g., Nuclear Regulatory Commission [NRC]), and International Organizations.

2.1 AFC Integration Meetings and Technical Workshops

L. Braase, lori.braase@inl.gov, INL

Three AFC integration meetings were conducted during FY 2012. In general, the meetings consisted of DOE-NE guidance, industry partner's needs and insights, and technical presentations that provided the status of R&D efforts. The meeting locations and dates are listed below.

- *Washington DC, October 25-27, 2011.* The nanotechnology 2012 effort was discussed during this meeting, leading to the two workshops discussed below. Along with technical status and planning presentations, a status was provided by the Separations and Waste Forms Task Force and industry representatives provided technical and strategic feedback to AFC.
- *Salt Lake City, UT, April 3-4, 2012.* This was an integrated meeting with the Separations and Waste Forms Campaign to discuss results of the Modified Open/Full Recycle Task Force. Short technical presentations were made to provide mid-year accomplishments status.
- *Los Alamos, NM, September 11-13, 2012.* Highlights of this meeting include discussions of Enhanced Accident Tolerant LWR Fuels development efforts, new AFC structure, advanced fuels related Nuclear Energy University Program (NEUP) presentations, and industry feedback.
- *2012 FCRD NanoNuclear Workshop, Smalley Institute of Nanoscience and Technology, Houston, Texas, February 28-March 1, 2012.* AFC provided the management and technical resources for this workshop, which brought the technical experts from universities, industry, and the FCRD program together to discuss issues, needs, and possibilities for nanoscience.

- *2012 NanoNuclear Workshop, June 6-8, 2012, Gaithersburg, Maryland.* This workshop was sponsored by DOE-NE and The Minerals, Metals, and Materials Society (TMS). AFC supported the management of the workshop as well as driving the technical outcomes. It was the third workshop, with a broader technical audience, to identify productive lines of research and approaches for nanotechnology in the nuclear research environment.

2.2 Interfaces

J. Carmack, jon.carmack@inl.gov, INL

The Advanced Fuel Campaign interfaces with a variety of DOE programs, commercial nuclear industry, and universities. The campaign maintains specific interfaces with the Light Water Reactor Sustainability (LWRS) Program and the Separations and Waste Forms Campaign. The LWR Accident Tolerant Fuels (ATF) effort includes strong collaborations with industry, Nuclear Regulatory Commission (NRC), international organizations, and the integrated programs across DOE-NE.

Late in FY-2012, three industry led projects were competitively awarded by the DOE-NE. In addition, two NEUP funded projects are under the direct responsibility of the AFC program. The University of Illinois Urbana-Champaign led project investigating modified zirconium cladding technology and the University of Tennessee led project investigating ceramic cladding coating technologies.

Three DOE Funding Opportunity Announcements (FOA) for industry-led projects were funded late in FY 2012. These industry projects are closely coordinated with AFC through directly funded DOE laboratory participation, as well as industry participation in AFC-led characterization and irradiation testing activities. It is expected that these three industry projects, which include participation by national laboratories and universities, will successfully identify potential accident tolerant fuel designs and concepts.

- Westinghouse Electric Corporation will investigate advanced cladding concepts coupled with advanced fuel pellet design.
- General Electric Corporation will investigate advanced cladding for enhanced accident tolerance.
- AREVA will investigate a number of fuel and cladding options ultimately choosing one for testing and development.

Two university-led, Integrated Research Proposals (IRP) were also funded late in FY 2012, to specifically develop accident tolerant fuel concepts. The University of Illinois Urbana-Champaign project will investigate modified zirconium cladding technology and the University of Tennessee project will investigate ceramic cladding coating technologies. They both support AFC's goal for R&D in accident tolerant fuels.

The Nuclear Education University Program (NEUP), under the direction of DOE's Office of Nuclear Energy (NE-4), funds multiple projects related to AFC. These projects are ongoing and range from the development of enhanced thermal conductivity fuel compositions to the development of advanced in-pile fuel testing methods and instrumentation. University programs and AFC continue to effectively collaborate to meet DOE's nuclear energy R&D goals.

2.2.1 LWR Fuels with Enhanced Accident Tolerance

Shannon Bragg-Sitton, INL

DOE-NE, in collaboration with the nuclear industry, has been conducting R&D activities on advanced LWR fuels for the last few years. Prior to the Fukushima event, the emphasis for DOE-NE

LWR R&D activities was on improving the fuel performance in terms of increased burnup for waste minimization, increased power density for power upgrades, and collaborations with industry on fuel reliability. This was an interface activity in 2012, but will be fully integrated into the Campaign in 2013.

After the Fukushima events in 2011, the emphasis shifted to accident performance of the fuels under extended loss of active cooling and steam exposure. Subsequently, the congressional appropriation language for FY 2012 included specific language for DOE-NE to initiate an aggressive research, development, and demonstration (RD&D) program for LWR fuels with enhanced accident tolerance. As a result, DOE-NE created a roadmap for the "Development of LWR Fuels with Enhanced Accident Tolerance," (release pending Congressional approval).

The mission of the Accident Tolerant Fuel (ATF) Roadmap is to develop the next generation of LWR fuels with improved performance, reliability, safety characteristics during normal operations, accident conditions, and reduced waste generation. To enhance the accident tolerance of fuel, initial RD&D efforts will focus on applications in operating reactors or reactors with design certifications. However, what we learn and develop during this process may be applicable to the design of the next generation of LWRs.

Fuels with enhanced accident tolerance are those that, in comparison with the standard UO_2 –Zircaloy system, can tolerate loss of active cooling in the core for a considerably longer time period (depending on the LWR system and accident scenario) while maintaining or improving the fuel performance during normal operations, operational transients, as well as design-basis and beyond design-basis events.

Design objectives already identified as potentially important to improve accident tolerance, include reduced hydrogen generation, improved fission product retention, improved cladding reaction to high-temperature steam, and improved fuel cladding interaction for improved performance under extreme conditions.

2.2.2 Fuels-Separations-Waste Forms Interface

E. Shaber, INL

The interface between AFC and the Separations and Waste Forms Campaign developed from the Advanced Fuel Cycle Facility design effort, which identified critical handoffs with separations that affected the fuel feed conditioning portion of fuel fabrication. Joint meetings between these campaigns have identified common technical issues, such as separations product conversion methods and development; fuel impurity specifications and requirements; fuel scrap recovery within separations; and fuel waste streams definition and analyses.

A Joint Task Force, "Reference Fuel Cycle Analysis and Comparison," was organized to provide a detailed comparison of the reference full recycle and limited recycle fuel cycles. (*INL/LTD-12-25400, Task Force Report, Reference Fuel Cycle Analysis and Comparison, July 2012*.) The task force defined reference fuel cycles with mass balances, efficiencies, waste generation, technical and regulatory issues and roadblocks, safety and security (nuclear material control and accountability) issues, technical unknowns, and research and development required.

2.3 International Collaborations

J. Carmack, jon.carmack@inl.gov, INL

AFC researchers are very active in international collaborations with Korea, France, Japan, China, Russia, and EURATOM. These interactions and collaborations are managed through a combination of participation in Generation IV Global International Forum projects, International Nuclear Energy Research Initiative (INERI) projects, and participation in bilateral and trilateral government-to-government agreements. The major international activities conducted in FY 2012 are summarized below:

2.3.1 Gen-IV GACID Project

J. Carmack, INL, K. McClellan, LANL

The Global Actinide Cycle International Demonstration (GACID) project seeks to demonstrate the irradiation and performance of minor actinide-bearing MOX fuel in the Monju reactor in Japan. Critical to this effort is the supply of feedstock materials needed to fabricate characterization samples and fuels for the irradiation tests. Recent events in Japan have changed funding priorities. In light of this, the GACID program and agreements are currently undergoing modification and renegotiation. Redefinition of the schedules and near terms goals of the program will be completed in FY 2013.

2.3.2 Gen-IV Advanced Fuel Project

K. McClellan, LANL, J. Carmack, INL

The Gen-IV Sodium Fast Reactor (SFR) project provides the means for collaboration on the development of advanced fuels for including metallic, ceramic, nitride, carbide, and advanced clad systems. The U.S. contributed updates on PIE of a subset of the ATR metal and oxide fuel irradiations and on advanced clad fabrications. Currently, the Russian Federation and the Republic of China are considering active participation in the project under the Gen-IV framework. Their specific contributions are currently being reviewed by the policy board for acceptance.

2.3.3 CEA-DOE Bilateral

K. Pasamehmetoglu, S. Hayes, INL

DOE and France's Atomic Energy Commission (CEA) are jointly pursuing the assessment of the UO_2-Am system as a transmutation system for americium. Researchers from DOE and CEA are currently studying the irradiation performance of an irradiation experiment testing this concept. The analyses of CEA and DOE will be shared and compared. This effort was initiated in FY 2009 and continued through FY 2012. Activities associated with design of an irradiation experiment for ATR will be completed in FY 2013. Additional tasks have been identified between CEA and DOE in 2012, including joint cladding development activities as well as coordination of the return shipment of the FUTURIX experiment to the U.S., currently planned for early 2013.

2.3.4 JAEA-DOE Bilateral Collaboration on Accident Behavior of Oxide Fuels

J. Carmack, INL, K. McClellan, LANL

Following the Fukushima event, the AFC ceramic fuels team and the Japan Atomic Energy Agency (JAEA) Tokai fuel property team began looking at opportunities for increased bilateral collaboration on accident behavior of oxide fuels. A number of areas for collaboration were identified and provided to the respective program management for potential inclusion in the DOE/JAEA bilateral and DOE/JAEA/CEA multilateral arrangements. Examples include performing joint oxidation studies of oxide materials, definition and information sharing on a joint DOE and Central Research Institute of Electric Power Industry (CRIEPI) metallic alloy fuel irradiation in Joyo, as well as the use of irradiation testing facilities.

An internationally recognized researcher from JAEA has been working collaboratively with researchers at LANL on oxidation kinetics of oxide fuel compositions during FY 2012. He was appointed a guest scientist to continue his research at LANL after losing his home in the earthquake. While JAEA is supporting the research, the experiments are aligned and coordinated with the ongoing AFC fundamental studies of oxidation behavior of UO_2 fuels including conditions relevant to off-normal and accident conditions.

2.3.5 EURATOM INERI Agreement

J.R. Kennedy, INL

EURATOM-DOE collaborative fuel R&D focused on specific technical staff exchanges on fabrication and characterization methods with the Joint Research Center-Institute of Transuranium Elements.

2.3.6 China Bilateral

K. Pasamehmetoglu, J. Carmack, INL

DOE and China Institute of Atomic Energy (CIAE) representatives meet in Beijing, China to discuss collaborative topical areas under the US-China Civil Nuclear bilateral Collaboration in August 2010 and again in Albuquerque, NM in September 2010. Following a bilateral meeting held in September 2012, the DOE and CIAE researchers have exchanged information on a potential materials irradiation test to be conducted in the Chinese Experimental Fast Reactor (CEFR) in 2014.

2.3.7 Russia Bilateral

J. Carmack, INL, S.A. Maloy, LANL

US-Russia Civil Nuclear Bilateral Collaboration has focused primarily on joint materials irradiation in BOR60, metallic alloy fuel development, characterization and PIE methods, in-pile instrumentation, and advanced LWR fuels. Most recently a subcontract was initiated by DOE with the Russian Research Institute of Atomic Reactors (RIAR) institute to begin design of a materials irradiation apparatus for BOR60.

2.3.8 OECD/NEA Expert Group on Innovative Fuels

K. Pasamehmetoglu, INL

The Innovative Fuels Expert Group, chaired by a U.S. representative, is currently working on publishing a state-of-the-art report on innovative fuels. In addition, the OECD/NEA is sponsoring an enhanced ATF metrics definition meeting in Paris, the week of December 10, 2012.

2.3.9 Republic of Korea CRADA and INERI Projects

J. R. Kennedy, INL, T.S. Byun, ORNL

In 2011, a new Cooperative Research and Development Agreement (CRADA) was signed between INL and the Korean Atomic Energy Research Institute (KAERI) to jointly conduct research and development on the recycle, fabrication, and irradiation of materials irradiated in a light water reactor. After processing and recycling used nuclear fuel at the INL Fuel Conditioning Facility, new fuel pins will be fabricated and irradiated in ATR. Work in this area progressed towards preparing for the fabrication of this irradiation test.

Two INERI projects are also being conducted jointly between U.S. researchers and KAERI researchers. The first led by Dr. T. S. Byun focuses on advanced cladding materials development and the second led by Dr. Rory Kennedy focuses on advanced metal fuel fabrication processes. These activities will help facilitate joint research and development between the U.S. and S. Korea and it is expected that significant interactions and collaborative activities will continue in 2013.

3. METALLIC BASED FUELS TECHNOLOGIES

J. R. Kennedy, rory.kennedy@inl.gov, INL

Metallic-based Fuels Technologies focused on research and development to gain a fundamental understanding of metallic fuels. Priority was on low-loss fabrication methods and capability and on developing a fundamental understanding of the phase, microstructure, and chemical migration behavior of metallic fuel constituents. The desired outcome is to develop an understanding of the key phenomena affecting metallic fuel performance and behavior under irradiation.

3.1 Thermoacoustic Sensor for In-pile Measurements

J. Smith, INL

An important investigative area of AFC is to develop sensors that can withstand the extremely harsh in-pile environment so that changes in the fuel can be monitored on a real time basis. Although most efforts in this area have been directed at adapting existing sensing technologies to the harsh environments of a reactor, the approach taken by the Thermoacoustic (TAC) sensor project is unique since it intends to take advantage of the harsh nuclear environment and maintain synergy between the sensor and the environment. To ensure the development of an effective in-pile device, the synergistic device must meet five necessary criteria:

1. Be synergistic with the in-pile environment
2. Demonstrate a useful function (sensing, enhance heat transfer)
3. Be wireless
4. Be self-powered indirectly from fuel or gamma heating with no moving parts
5. Have a form factor that can be inserted into a reactor environment.

A TAC engine (Figure 1) takes advantage of the thermal gradients within a reactor core to power an acoustic jet stream within a gas filled resonator (fuel capsule). The TAC engine can be built from the same materials used to construct the core and fuel assemblies. The resonant acoustic tone generated by the TAC engine is the wireless communication mechanism to transmit the measurement signal. The TAC project has demonstrated acoustic transmission through water and through metal conduit/piping that is representative of materials found in reactor cores.

Experimental results, using laboratory mockups, have demonstrated the merits of thermoacoustic devices for *in-situ* use. A number of sensors (temperature, material expansion, pressure, etc.) have been designed from TAC engines and have demonstrated excellent resolution. TAC engines have also been configured to differentiate various microstructure related parameters such as porosity, surface conditions, and fission gas composition. A TAC engine has been demonstrated with a form factor capable of being inserted into a materials test reactor. It is also shown that acoustic waves generated by the TAC device can be remotely analyzed and correlated to porosity state changes in materials (Figure 2). Thus, the TAC engine has been demonstrated to meet all five criteria.

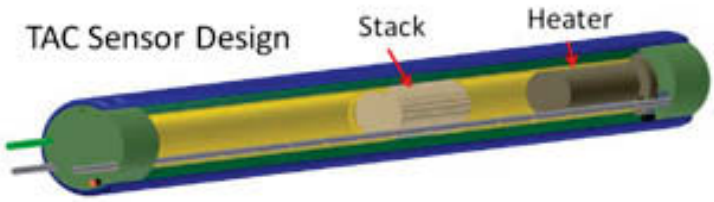

Figure 1. The TAC heat pump is powered by the temperature differential across the stack. In this embodiment, the stack is Celcor®, a ceramic material, usually used as a substrate for automotive catalytic converters, with 1,100 parallel square pores per square inch.

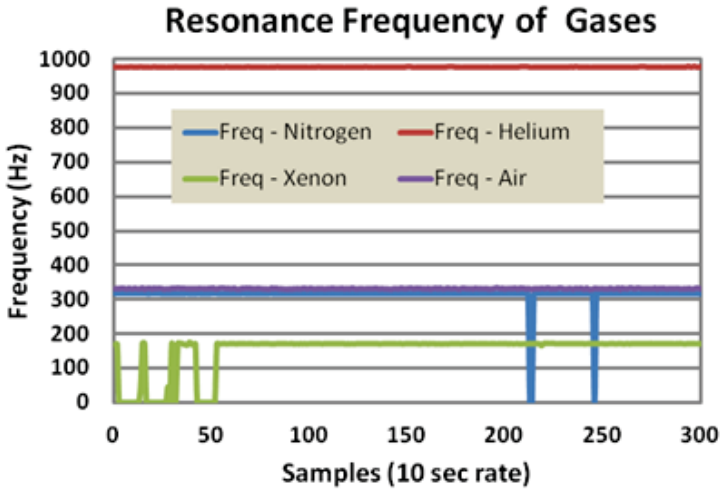

Figure 2. Plot showing the experimental results to demonstrate the direct correlation between the resonance frequency and the mean molecular mass of a gas. The resulting frequencies are properly ordered based on molecular weight.

PATENTS AND INVENTIONS DISCLOSURE REPORTS (IDR):

[1]. S. L. Garrett, J. A. Smith, and D. K. Kotter, "Thermoacoustic Enhancements for Nuclear Fuel Rods", U. S. Provisional Pat. App. No. 61/683,992 (filed 16 Aug 2012).

[2]. Rick Oran Parry, James Arthur Smith, Dale Kent Kotter, BA-751 2262, Modeling of material microstructure, 7/11/2012.

[3]. James Arthur Smith, Dale Kent Kotter, Steven Garrett, BA-736 2245, Method to Enhance Nuclear Fuel Heat Transfer, 5/7/2012.

3.2 Laser-based Characterization/PIE Technique Development

D. Hurley, INL

Two key accomplishments were achieved in the advancement of laser-based techniques to determine mechanical and thermal properties of nuclear fuel and these are the Thermal Properties Microscope and the Mechanical Properties Microscope.

3.2.1 Thermal Property Microscope (TPM)

This laser based instrument will allow the determination of thermal conductivity through the direct measurement of thermal diffusivity and thermal effusivity. The thermal conductivity can be extracted

from these two measurements. The determination of the thermal conductivity in this way is important because it alleviates the need to separately measure the specific heat, which is rather difficult under remote handled conditions. The instrument is being designed so that it can be remotely operated and maintained, will function in a radiation environment, and can make measurements on nuclear fuel and other radioactive samples. Once operational, this instrument will provide micron-level thermal property information that is commensurate with the microstructure heterogeneity in nuclear fuel.

The following is a list of key accomplishments pertaining to the design, construction, and testing of the TPM:

- Developed an experimental protocol appropriate for measuring thermal conductivity of high burnup nuclear fuel as well as fresh nuclear fuel.
- Completed a study on the suitability using a fiber laser for sample heating.
- Identified a figure of merit that can be used to judge data reliability.

The values for the effusivity, thermal diffusivity, and thermal conductivity obtained on metallic systems from the Thermal Conductivity Microscope (TCM) compare very well with those known from the literature. Of particular note is the rather good correspondence between literature values and TCM determined values for ceramic materials as demonstrated with the data listed in Table 1.

Table 1. Comparison of the effusivity, thermal diffusivity, and thermal conductivity values determined with the TCM for SiO2 and CaF2 with literature values.

	Sample A (SiO_2)	**Sample B (CaF_2)**
Phase lag (deg)	60.4	46.3
Effusivity ($J/m^2\ s^{1/2}\ K$), measured	1490	4570
Effusivity ($J/m^2\ s^{1/2}\ K$), literature	1436	4989
Effusivity error	<4%	~8%
Diffusivity (m^2/s), measured	9.80×10^{-7}	3.25×10^{-6}
Diffusivity (m^2/s), literature	9.5×10^{-7}	3.4×10^{-6}
Diffusivity error	3%	4%
Conductivity (W/(m K), measured	1.47	8.24
Conductivity (W/(m K), literature	1.4	9.2
Conductivity error	5%	10%
Effusivity ($J/m^2\ s^{1/2}\ K$), measured including $R_{th} = 5 \times 10^{-9}\ m^2\ K/W$	1460	4180

3.2.2 Mechanical Properties Microscope (MPM)

The Mechanical Properties Microscope (MPM) is designed to operate in a hot cell environment via remote control manipulation and mockup testing of this unique laser ultrasound instrument to measure mechanical properties of nuclear fuel was initiated. The MPM will provide micron-level mechanical property information that is commensurate with microstructure heterogeneity. The spatial resolution of the MPM enables results to be tied directly with other electron/photon microstructural imaging technologies. This aspect is essential to understanding the role of microstructure in determining mechanical properties of nuclear fuel. Experimental results from the MPM were used as the cover illustration of the IEEE-UFFC Nov. 2012 issue (Figure 3).

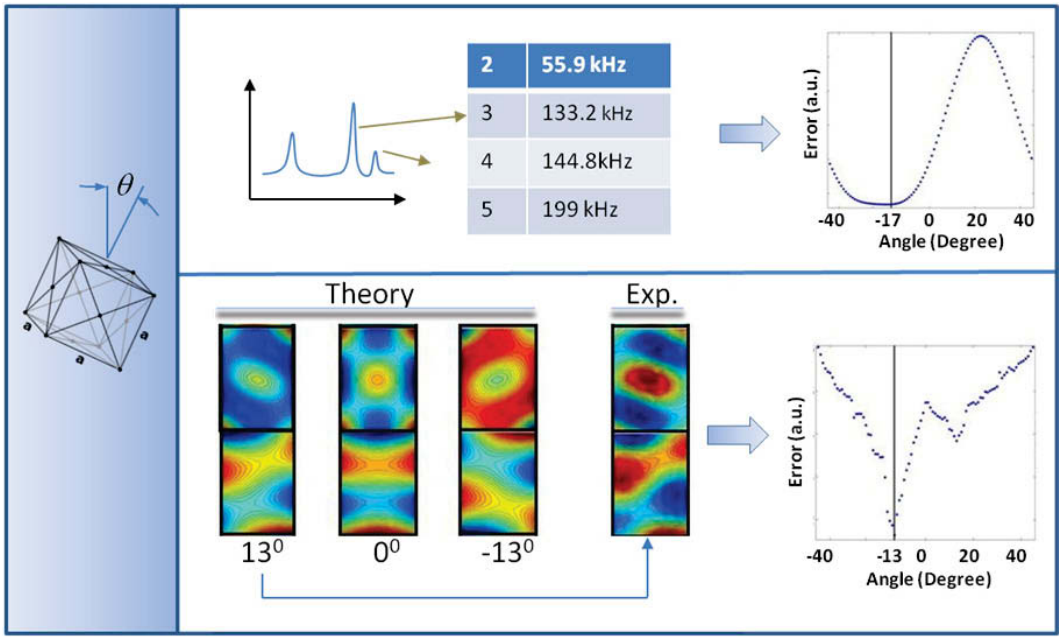

Figure 3. Cover illustration for the Nov. 2012 issue of IEEE-UFFC. The MPM was used to measure crystallographic orientation of a single crystal sample. Laser resonant ultrasonic spectroscopy (LRUS) uses lasers to excite and detect resonant modes. The crystallographic orientation of a copper sample determined using the eigenmode method (bottom) is compared with the traditional eigenfrequency method (top).

A number of important steps were completed on the path to remote operation implementation of the MPM including obtaining final approval of the remote equipment qualification plan for phase I testing, finalizing construction of the prototype instrument, and completing initial mockup testing. In addition, the first time measurement of the elastic constants of a cast U-Mo fuel ingot compared to a textured U-Mo fuel plate imposed by rolling (Table 2).

Table 2**.** Comparison of the first time measured elastic constants of a cast U-Mo fuel alloy with a rolled textured sample.

	Isotropic Ingot	Anisotropic rolled foil	Percent change
Young's Modulus (Gpa)	102	71	30
Shear Modulus	36	25	30

PUBLICATIONS:

[1]. F. Farzbod and D. H. Hurley, "Resonant Ultrasound Spectroscopy: Using Mode Shapes," IEEE Transactions on Ultrasonics, Ferroelectrics, and Frequency Control, to appear in Vol. **59**, No. 11, November 2012

[2]. Z. Hua, Heng Ban, M. Khafizov, R. Schley, J. R. Kennedy, D. H. Hurley, Spatially localized measurement of thermal conductivity using a hybrid photothermal technique, Journal of Applied Physics, **111** (2012).

[3]. D. H. Hurley, S. J. Reese, F. Farzbod, Application of laser-based resonant ultrasound spectroscopy to study texture in copper, Journal of Applied Physics, **111**, 53527 (2012).

COLLABORATIONS:

[1]. Utah State University

3.3 Remote Fuel Fabrication Development

R. Fielding, INL

In support of the Joint Fuel Cycle Studies (JFCS) CRADA with the Korean Atomic Energy Research Institute (KEARI), and more specifically the Integrated Recycle Test (IRT), fuel fabrication must be designed and implemented for remote operation under hot cell conditions. The IRT will recycle used light water reactor fuel into metallic feedstock for a fast reactor type fuel that will be irradiation tested in ATR. To this end, a versatile remote casting furnace used to produce the fuel alloy slugs has been designed (Figure 4a), a remote settler/bonder system used to ensure the fabricated fuel slugs are properly positioned in the cladding and completely engulfed and bonded with sodium has been designed (Figure 4b), a welding system used to weld the end caps to the cladding tube has been down selected and parametrically studied with various end plug designs (Figure 4c), and a comparison between two weld and sodium bond inspection systems performed (Figure 5).

The remote casting furnace will be able to function in a gravity casting mode or counter gravity injection casting mode and produce between one and six pins at lengths of up to 10 inches. The settler/bonder heats the loaded fuel rodlet while strike impacting the rodlet to settle the fuel slug to the bottom of the cladding and remove any void in the sodium from the fuel-clad gap. The impacting force is adjustable. Four welding systems, required for both the primary (rodlet) and secondary (capsule) cladding end capping, were studied and scored for cost, efficiency, and ease of use (technical readiness level) under remote handling conditions. These included Gas-Tungsten-Arc Welding (GTAW) orbital welding, GTAW burst welding, resistance pressure welding, and laser welding. GTAW burst welding scored as the preferred method and a mock-up system fabricated (Figure 4c) for a parametric study on weld results from various end cap designs. Finally, for reactor fuel qualification, two weld and sodium bond inspection systems were studied: a digital x-ray radiography using a microfocus x-ray source system and an ultrasonics based system. Standard x-ray radiography has been used extensively for fuel elements in the past. Ultrasonics has not been used for fuel elements but is standard in the construction and joining industries. The ultrasonic system may offer a number of advantages over the x-ray system, including ease of use and sensitivity, but more development is needed for hot cell applications. A comparison of the results from each technique on a sodium bonded fuel rodlet is shown in Figure 5.

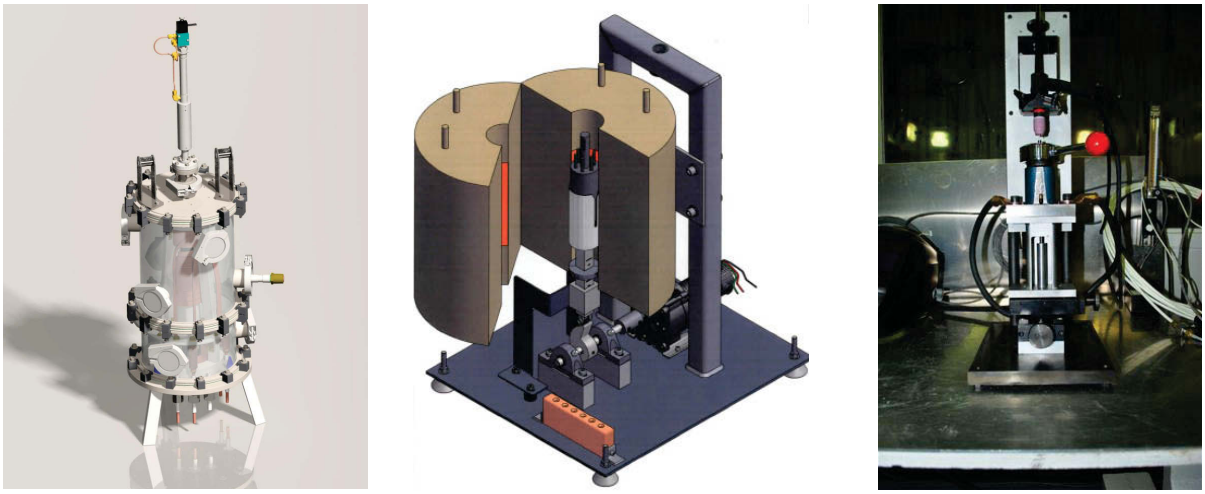

(a) (b) (c)

Figure 4**. (a)** Design model of JFCS casting furnace. (**b)** Design model of the settler/bonder. (**c)** Mock-up developmental welding system.

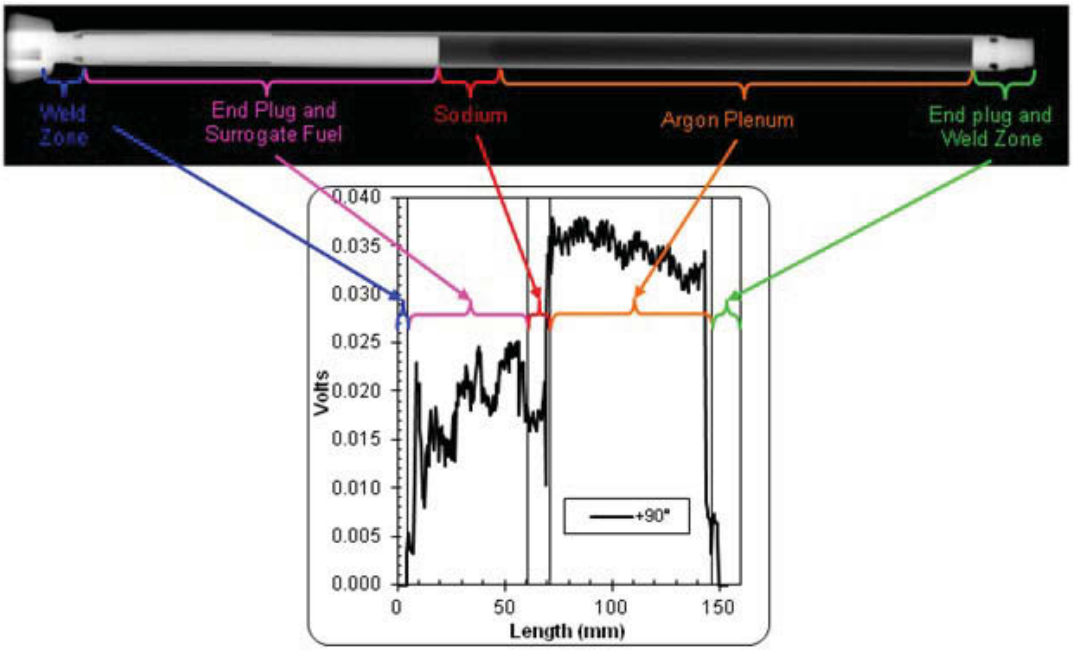

Figure 5. Sodium containing rodlet comparison of x-ray image (top) to ultrasonic data (bottom).

3.4 Innovative Metallic Fuels for Fast Reactors

R. Mariani, INL

Two approaches are being taken to improve the chemical stability of metallic nuclear fuel in order to extend fuel reliability to ultra-high burnup and to facilitate transuranic burning: 1) investigation of novel uranium based alloys with low body-centered-cubic (bcc) onset temperature coupled with higher melting temperatures and 2) addition of additives to the fuel to stabilize lanthanide fission products towards migration and fuel-cladding-chemical interaction (FCCI). Analyses and experiments have shown that the incorporation of each of the proposed alloy modifications is compatible with existing processes, such as fabrication and electrorefining.

In the first approach, novel uranium alloy systems suitable for burning transuranics were identified by thermodynamic analysis, with low onset temperature for cubic phase and higher melting temperature, and were corroborated by traditional alloy theory. Recent experimental evidence supports the hypothesis (Figure 6) and continued testing is designed to show that the safety margin for TRU bearing alloys will be increased and the in-pile fuel properties have a greater radial uniformity.

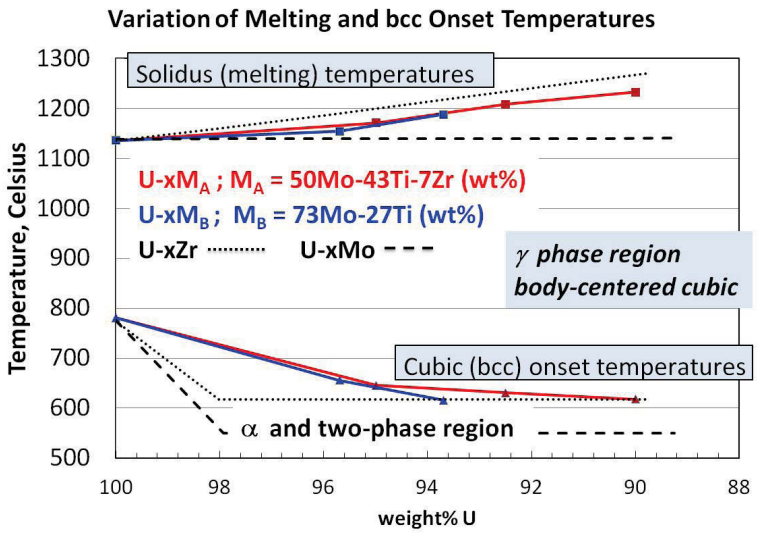

Figure 6. Key alloy characteristics for U-Zr, U-Mo, and novel systems showing increase in solidus temperatures and decrease in bcc onset temperatures.

In the second approach, the criteria for selection of additives to stabilize lanthanide fission products were first identified. It is known that lanthanide fission products can migrate to the fuel-clad interface and enhance FCCI (Figure 7). Solid evidence was found to show how palladium effectively binds the lanthanide fission products and inhibits FCCI (Figure 8). As a result, contamination from lanthanide carryover in electrorefined uranium and transuranics can be managed and higher burnups can be expected, perhaps on the order of 20 atom percent.

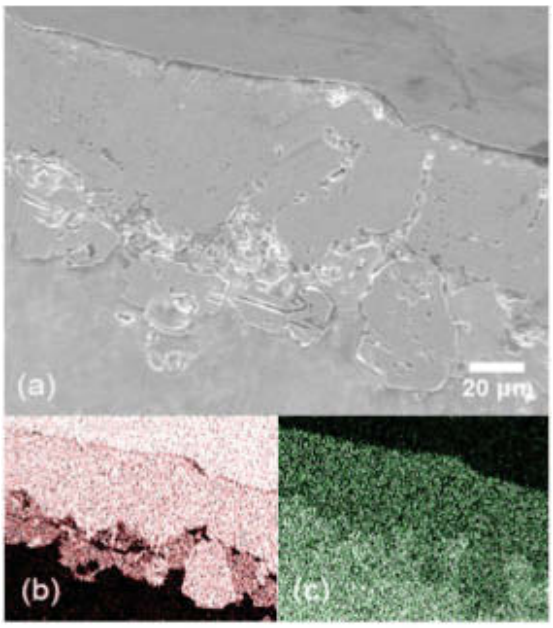

Figure 7. (a) SEM backscattered electron image of results from a diffusion couple between Fe (red in (b) x-ray map) and a representative lanthanide fission product Nd (green in (c) x-ray map heated to 700°C. Significant interdiffusion is observed.

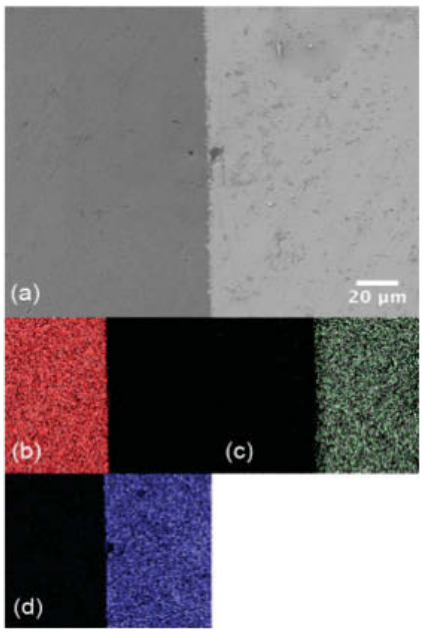

Figure 8. (a) SEM backscattered electron image of results from a diffusion couple heated to 700°C between Fe (red in (b) x-ray map) and a Pd-Nd alloy. Nd is green in (c) x-ray map and Pd is blue in (d) x-ray map. No interdiffusion is observed.

PUBLICATIONS:

[1]. R.D. Mariani, D.L. Porter, T.P O'Holleran, S.L. Hayes, and J.R. Kennedy. Lanthanides in metallic nuclear fuels: their behavior and methods for their control. J. Nucl. Materials 2011; 419: 263-271.

[2]. G.W. Egeland, R.D. Mariani, T. Hartmann, D.L. Porter, S.L. Hayes, and J.R. Kennedy. Reducing fuel-cladding chemical interaction: The effect of palladium on the reactivity of neodymium on iron in diffusion couples. J. Nucl. Materials 2012, in press, doi: http://dx.doi.org/10.1016/j.jnucmat.2012.07.028.

PROCEEDINGS:

[1]. A.E. Wright, S.L. Hayes, T.H. Bauer, H.J. Chichester, G.L. Hofman, and J.R. Kennedy, et al. Nuclear fuel and structural materials for the next generation nuclear reactors, In: Transactions of the American Nuclear Society, Embedded Topical on Nuclear Fuel and Structural Materials, American Nuclear Society, Chicago, IL: American Nuclear Society; 2012: 1102-1105.

[2]. R.D. Mariani, D.L. Porter, S.L. Hayes, and J.R. Kennedy. Chemical stabilization of metallic nuclear fuels. In: Transactions of the American Nuclear Society, Embedded Topical on Nuclear Fuel and Structural Materials, Chicago, IL: American Nuclear Society; 2012: 1098-1101.

[3]. R.D. Mariani, D.L. Porter, S.L. Hayes, and J.R. Kennedy. Metallic Fuels: The EBR-II Legacy and Recent Advances, Proceedings of the ATALANTE 2012: Nuclear Chemistry for Sustainable Fuel Cycles, Montpellier, France, September 2012, Procedia Chemistry, in press.

[4]. V. Blackwood, T.W. Koenig, J.M. Porter, D.L. Olson, B. Mishra, and R.D. Mariani, et al. Elemental solubility tendency for the phases of uranium by classical models used to predict alloy behavior. In: Symposium on the Materials and Fuels for the Current and Advance Nuclear Reactors, Orlando, FL: TMS; 2012.

[5]. G.W. Egeland, T. Hartmann, R.D. Mariani, and D.L. Porter. Effects of metal additives on lanthanide fission product interactions with cladding iron: out-of-pile transport studies. In: Symposium on the Materials and Fuels for the Current and Advance Nuclear Reactors, Orlando, FL: TMS; 2012.

[6]. H.J. Chichester, R.D. Mariani, S.L. Hayes, J.R. Kennedy, A.E. Wright, and Y.S. Kim, et al. Advanced metallic fuel for ultra-high burnup: irradiation tests in ATR. In: Transactions of the American Nuclear Society, Embedded Topical on Nuclear Fuel and Structural Materials, Chicago, IL: American Nuclear Society; 2012: 1349-1351.

COLLABORATIONS:

[1]. Colorado School of Mines

[2]. University of Nevada, Las Vegas

3.5 Neutronic Effects of Additives

T. K. Kim, A. Wright, ANL

The reactor-core neutronic effects of including additives in as-fabricated fuel to help prevent cladding attack by lanthanide fission products was evaluated on the basis of a reference 3000 MWth homogeneous ultra-high burnup reactor (UHBR) core, fueled with ternary U-TRU-10Mo alloy in which the TRU has been recovered from used LWR fuel. Charge fuel was assumed to have composition U-TRU-X-10Mo, with X being the additive element. Adjustments in fissionable content were made in the mass fraction of TRU to total heavy metal (HM) to compensate for the inclusion of the additive. The base case (no additives) has a TRU/HM mass ratio ("TRU enrichment") of 18% and a burn cycle length of 810 days with eight-batch fuel management scheme, which results in an average discharge burnup of 32%. Two additives were evaluated: palladium (Pd) and indium (In). Both have about the same neutron capture cross

section (per atom) in the UHBR environment, but Pd has a higher mass density (12.0 g/cc) and thus a lower atom density compared to In (7.3 g/cc). The neutronic penalty (capture cross section times atom density) of In is thus about 1.6 times that of Pd. Adding the additives leads to an increase in TRU enrichment or a decrease in discharge burnup, and the additive concentration is limited by both the target discharge burnup and the maximum excess reactivity that could be suppressed by the primary control rods in adequate safety conditions. To achieve a similar discharge burnup as in the base case, an addition of ~4% Pd or ~3% In would be near the limit of additive concentration, which requires an increase in TRU enrichment (by a factor of about 1.4 to 1.5, in either case) to compensate for the penalty of the additives. Alternatively, keeping the same 18% TRU enrichment as in the base case, and adding 4% Pd or 3% In, the burn cycle length would need to be decreased by about 30%.

PROCEEDINGS:

[1]. T. K. Kim and A. E. Wright, "Development of Advanced Ultra-High Burnup SFR Metallic Fuel Concept – Impacts on Core Characteristics and Fuel Cycle Performance," Trans. Am. Nucl. Soc. 106 (2012) 1362-1363. Trans. Am. Nucl. Soc. 106 (2012) 1098-1101.

3.6 Fundamental Fuel-Cladding-Chemical-Interaction Studies

B. Sencer, INL

This project is to provide an understanding of thermally-activated and irradiation-enhanced multicomponent-multiphase diffusion including relevant microstructural evolution in components of the U-Zr-Ln and U-Mo-Ln systems in contact with Fe and Fe-Cr alloys. The results from these studies will provide critical thermokinetic data and microstructural information for multiscale modeling of the fuel-cladding interaction (FCCI), and at the same time, validate the results of FCCI modeling.

By studying diffusion in a series of binary and higher order diffusion couples, both solid-to-solid and thin film (started recently), kinetic coefficients can be determined for species ranging from impurity to multicomponent intrinsic/interdiffusion coefficients. To this end, the development of the microstructure (e.g., phase identification and concentration profiles) was examined using state-of-the-art instrumentation and innovative analytical methods. Specific systems studied included Mo vs. Zr, Mo vs. Fe and Fe alloys, Zr vs. Fe and Fe alloys, Ce vs. Fe and Fe alloys, Nd vs. Fe and Fe alloys, U vs. Fe and Fe alloys, U-10Zr vs. Fe and Fe alloys, U vs. Mo, U-10Zr vs. Mo, U vs. Zr, U-10Zr vs. Zr, U vs. Ce, U-10Zr vs. Ce, U vs. Nd, and U-10Zr vs. Nd were investigated via solid to solid diffusion couples.

An example of an examined diffusion couple system for U vs. Fe is given below. Here, diffusion couples were annealed at temperatures in both the α-U temperature range (580, 615, and 650°C) and β-U temperature range (680 and 700°C). Back-scattered electron (BSE) images and averaged concentration profiles of diffusion couples at 650K are shown in Figure 9.

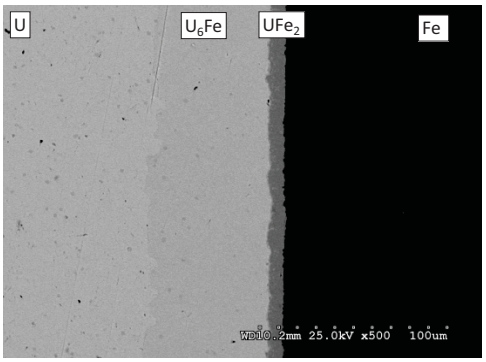

(a)

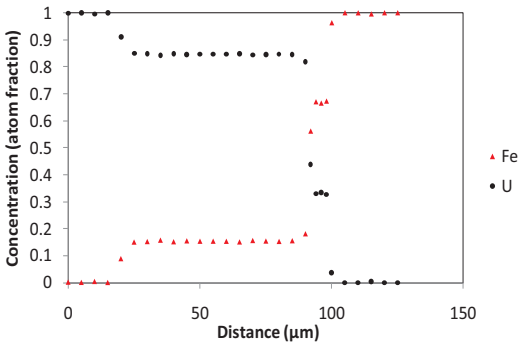

(b)

Figure 9. Backscatter electron micrograph and concentration profile of U vs. Fe diffusion couple annealed at 650°C for 4 days.

The 4 phases presented in Figure 9a are pure U, U_6Fe, UFe_2 and pure Fe from the left to the right side, which corresponds to the equilibrium phase diagram very well. The interfaces between each phase are uniform and planar. Integrated interdiffusion coefficients $\tilde{D}^{Int}$ (Table 3), first kind growth constants ("extrinsic") K_I (Table 4), and second kind growth constants ("intrinsic") K_{II} (Table 5) were determined. The differences in activation energies for each phase between the α-U temperature range and the β-U temperature range are small, which indicates the allotropic transformation of U plays only a small role in the growth of U_6Fe and UFe_2.

Table 3. Integrated interdiffusion coefficients of U_6Fe and UFe_2 in α-U and β-U terminal ends.

U Phase	T (K)	$\tilde{D}^{Int,U_6Fe}$ (x10^{-16} at. frac. m^2/s)	$Q^{\tilde{D}^{Int,U_6Fe}}$ (KJ/mol)	$\tilde{D}^{Int,UFe_2}$ (x10^{-16} at. frac. m^2/s)	$Q^{\tilde{D}^{Int,UFe_2}}$ (KJ/mol)
α-U (orthorhombic)	853	1.56	148.46	0.040	243.37
	888	3.60		0.162	
	923	7.63		0.534	
β-U (tetragonal)	953	11.35	112.73	0.680	225.97
	973	15.21		1.22	

Table 4. Type one parabolic growth constant ("extrinsic") of U_6Fe and UFe_2 in α-U and β-U terminal ends.

U Phase	T (K)	$K_I^{U_6Fe}$ (x10^{-16} m^2 /s)	$Q^{K_I^{U_6Fe}}$ (KJ/mol)	$K_I^{UFe_2}$ (x10^{-16} m^2/s)	$Q^{K_I^{UFe_2}}$ (KJ/mol)
α-U (orthorhombic)	853	12.46	146.08	0.036	298.57
	888	28.44		0.208	
	923	59.44		0.880	
β-U (tetragonal)	953	88.93	108.89	1.021	281.23
	973	117.97		2.118	

Table 5. Type two parabolic growth constant ("intrinsic") of U_6Fe and UFe_2 in α-U and β-U terminal ends.

U Phase	T (K)	$K_{II}^{U_6Fe}$ (x10^{-16} m^2 /s)	$Q^{K_{II}^{U_6Fe}}$ (KJ/mol)	$K_{II}^{UFe_2}$ (x10^{-16} m^2/s)	$Q^{K_{II}^{UFe_2}}$ (KJ/mol)
α-U (orthorhombic)	853	13.88	148.46	0.196	243.37
	888	32.05		0.797	
	923	67.91		2.652	
β-U (tetragonal)	953	101.05	112.73	3.342	225.97
	973	135.40		6.008	

PUBLICATIONS:

[1]. Michael T. Myers, Bulent H. Sencer, Lin Shao, "Multi-scale modeling of localized heating caused by ion bombardment" Nucl. Instr. and Meth. in Phys. Res. B (2012) 165-168.

[2]. K. Huang, Y. Park, A. Ewh, B.H. Sencer, J.R. Kennedy, K.R. Coffey, Y.H. Sohn, "Interdiffusion and reaction between uranium and iron" Journal of Nuclear Materials 424 (2012) 82–88.

[3]. Chao-Chen Wei, Assel Aitkaliyeva, Zhiping Luo, Ashley Ewh, Y.H. Sohn, J.R. Kennedy,

[4]. Bulent H. Sencer, M.T. Myers, M. Martin, J. Wallace, M.J. General, Lin Shao, "Understanding the Phase Equilibrium and Irradiation Effects on the Fe-Zr System: New Insights from the Diffusion Couple" Journal of Nuclear Materials, 432 (2013) 205–211.

COLLABORATIONS:

[1]. University of Central Florida

[2]. Texas A&M University

[3]. Georgia Institute of Technology

4. CERAMIC BASED FUELS TECHNOLOGIES

K. McClellan, kmcclellan@lanl.gov, LANL

Ceramic fuel development for FY2012 focused on oxide fuel and was a balance of effort seeking transformational R&D while incrementally advancing fuel technology. The fundamental, science-based approach employed in this area relies upon close coordination of theoretical, experimental and modeling efforts and that coordination is dependent upon separate effects testing (SET).

FY2012 work was structured around the fact that the key issues for establishing low loss processing and improved fuel performance are materials issues. Due to limited resources, the program has targeted urania-based oxide fuels with focus on LWR application. In light of the Fukushima Daiichi nuclear disaster, additional emphasis was placed upon increasing the ability to understand and improve the accident behavior of LWR fuel.

Key challenges targeted were the development of reliable, low-loss fuel fabrication methods, and development of fuel technology to enable major increases in fuel performance (safety, reliability, power and burn-up) beyond current technologies. Ceramic fuel development activities fell within the areas of 1) National and International Technical Integration, 2) Advanced Fuel Processing Development, 3) Property Determination and Advanced Characterization, 4) Fuel Performance and Separate Effects Testing, and 5) Reference Material and Technique Development. Significant accomplishments in the broad areas of processing, properties and performance for FY2012 include:

- Transitioned to a science-based approach for ceramic fuel development with a focus on separate effects testing involving close coordination between theory, experiment and modeling efforts. Key areas where the experimental program is now well positioned to provide necessary data sets for predictive model development include fuel pellet sintering, fission gas bubble formation, thermal conductivity, and single crystal properties.
- Melt point determination capability has been recaptured for materials up to ~3000 °C. This capability was demonstrated for five different urania-rare earth oxide compositions in the stoichiometric condition to provide a data set for model development and validation.
- A simultaneous thermal analysis system for measurement of the oxidation of uranium dioxide in controlled atmospheres containing up to 100% water vapor has been developed in collaboration with JAEA. The technique is capable of measuring oxidation of LWR fuels in situ during exposure to accident relevant environments at temperatures up to 1250°C.
- Near net shape sintering of UO_2 has been demonstrated to a tolerance of better than ±20 μm.
- A pellet measurement system has been demonstrated which provides 3-D mapping of green and sintered pellets along with a full pellet surface image that can be analyzed to identify defects (e.g. cracks and chips) in sintered pellets and which can be used for process monitoring via green pellet monitoring.
- An Ion Beam Assisted Deposition (IBAD) process has been demonstrated for producing thick films of UO_2 with xenon in solution without irradiation. Post synthesis annealing was shown to yield xenon bubbles that have dimensions and morphologies closely resembling those seen in irradiated fuels. These films demonstrated that samples can be fabricated to evaluate xenon behavior in UO_2 to simulate fission gas accumulation to facilitate development of fission gas models and act as a model system for SET experiments.
- Established co-conversion synthesis capabilities for reference oxide powder feedstocks, fabricated feedstock batches for separate effects, processing and properties studies.

- Powder conditioning and processing studies were performed for reference urania powder and the reference, co-converted feedstocks. These studies improved pellet quality and reliability and provided material for subsequent oxide fuel structure/property relations studies.
- Thermal transport studies were performed on various urania-based reference compositions providing fundamental data for development of improved thermal conductivity models.
- The first set of urania samples were fabricated in preparation for the first ceramic rabbit SET test in HFIR on thermal conductivity.

Reference single crystals of urania and urania compounds were grown by Bridgman and exaggerated grain growth methods.

4.1 Advanced Fuel Processing Development

4.1.1 Dimensional Control of Oxide Fuel Pellets

E. Luther, LANL

There are two major reasons for increasing our understanding of the sintering of ceramic oxide fuel pellets: 1) enhanced performance and 2) reduced waste. These goals are achieved by controlling the powder processing techniques used to fabricate fuel pellets by the conventional "cold press and sinter" approach currently used by the industry to mass produce pellets for the commercial LWR industry. The concept is that improved processing results in pellets with more uniform powder packing which necessarily shrink more uniformly during sintering and consequently have more uniform microstructures with fewer defects that will perform more reliably in-pile.

Urania powder was made to pack more uniformly by powder conditioning steps intended to minimize defects in the powder that disrupt packing and minimize frictional forces between particles which are the source of density gradients. Figure 10 is a plot of a pellet that was fabricated from powder that has been conditioned showing the extent of hourglassing has been significantly minimized. The maximum diameter variation has been decreased to 22 microns for the green pellet and 33 microns for the sintered pellet. This compares favorably with a dimensional tolerance specification of 25 microns for LWR pellets. The dimensional characterization is performed using a VISION system that is described in a companion highlight.

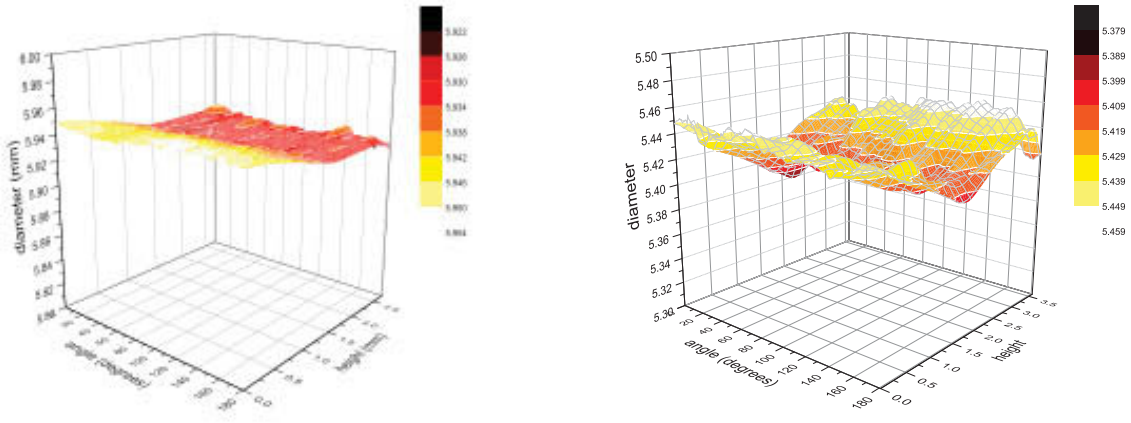

(a) (b)

Figure 10. Plots showing reduced diameter variation (33 μm) of a sintered pellet made from conditioned powder relative to that of as-received powder (68 μm).

4.1.2 VISION System for Automated Dimensional Characterization and Quality Control of Fuel Pellets

E. Luther, LANL

In order to accurately measure dimensional changes due to sintering, a Vision system was constructed. The system uses a highly accurate light-emitting diode (LED) micrometer to measure the diameter of the pellet as a function of height and angular position. Pellets can be measured in their green and sintered states observe shrinkage due to sintering. This provides an invaluable tool to determine improvements that are made to powder processing techniques during research and development.

Similar systems could be used in production environments for quality control. In Figure 11, an optical strip images is compared with the diameter surface map. The scale bar is in millimeters. Not only is a chip in the top of the pellet clearly observed in both the optical strip and diameter surface map, the magnitude of the chip can be assessed. In this instance, the chip is seen to be significant (~0.1 mm) which would indicate that the pellet should be rejected.

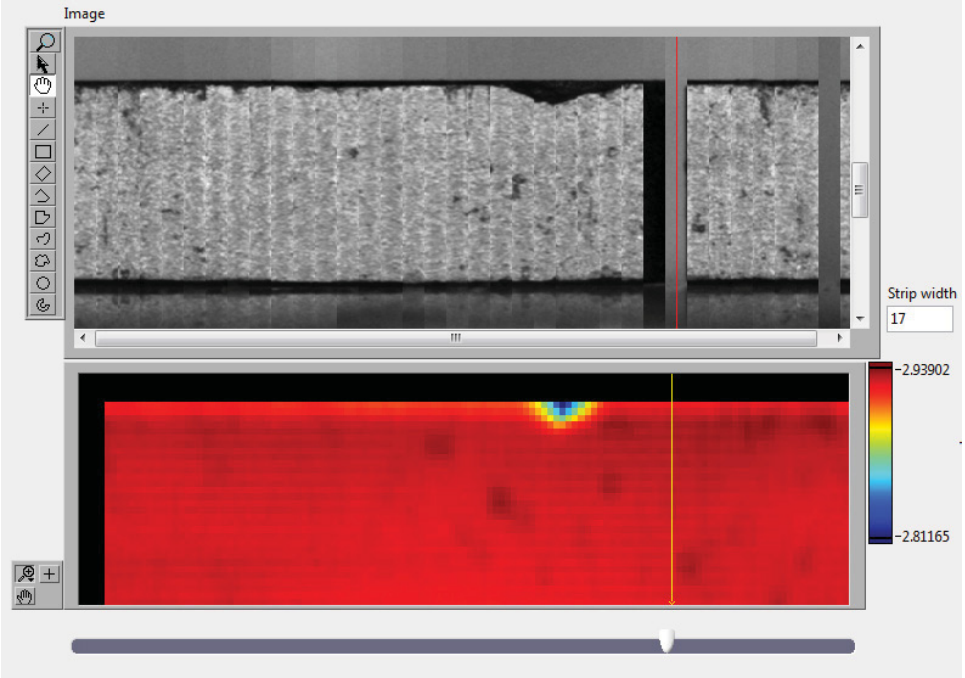

Figure 11. Optical "strip" map and corresponding diameter surface map showing chip in a fuel pellet.

An additional aspect of process control can be realized noting that the system can detect die degradation during pellet manufacture allowing the production facility to proactively replace dies showing unacceptable wear.

4.1.3 Direct Conversion of Mixed Uranium Lanthanide Oxides

S. Voit, R. Vedder, ORNL

During FY2012, synthesis of four batches of urania-gadolinia ($U_{98.5}Gd_{1.5}O_x$, $U_{97}Gd_3O_x$, $U_{95}Gd_5O_x$, $U_{88}Gd_{12}O_x$) and two batches of urania-thoria ($U_{95}Th_5O_x$, $U_{80}Th_{20}O_x$) were completed. The oxide feedstock preparation was performed using the Modified Direct Denitration (MDD) process which utilizes a heated rotary kiln to thermally denitrate double salts of ammonium and metals to produce powders ideally suited for thermophysical and thermochemical property measurements. The product powder has been packaged and is being shipped to LANL for use in fuel development studies.

Although the MDD process has been successfully used in the direct conversion of mixed metal nitrate feeds producing $(U,Ln)O_2$ and $(U,Pu,Np)O_2$ solid solutions, a substantial amount of development is

needed to provide a better understanding of the relationships between process parameters and product powder properties. Figure 12 shows a diagram of the internal components of the MDD rotary kiln and the measured temperature profile during denitration.

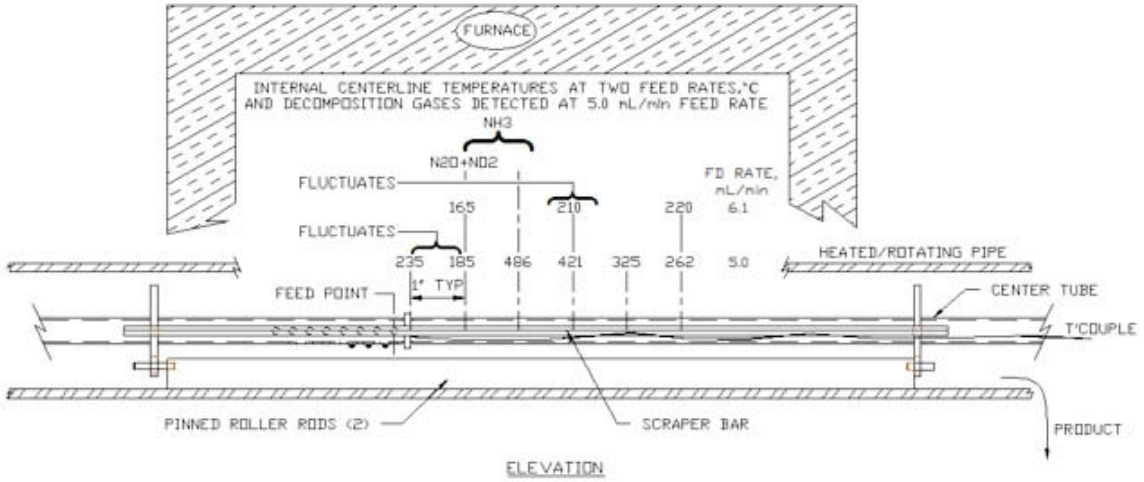

Figure 12. Temperature profile in MDD kiln during thermal denitration.

4.1.4 Spherical Particle Technology Research for Advanced Nuclear Fuel/Target Applications – INERI

S. Voit, I. Dunbar, C. Silva, ORNL

Under the International Nuclear Energy Research Initiative (INERI) Program, the DOE and the Institute for Transuranium Elements (ITU) are collaborating on spherical particle technology research. In FY2012, studies have focused on pressing and sintering characteristics of porous UO_2 particles made using the sol-gel process.

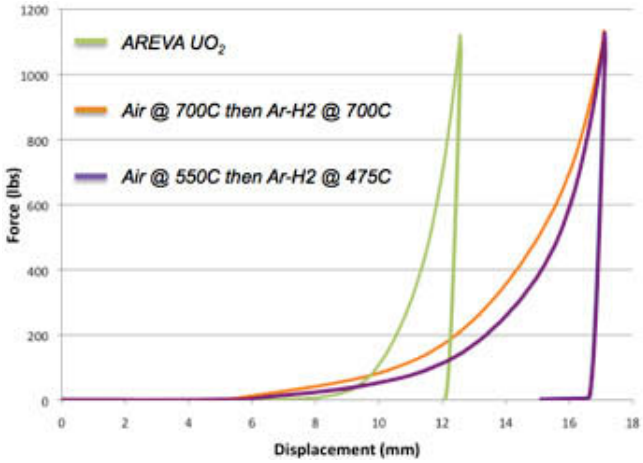

Figure 13. Compression curves for porous UO_2 spherical particles.

The force versus displacement data in Figure 13 show that UO_2 spheres that have been calcined at higher temperature require a greater force to achieve a given displacement and the pressing stroke is much longer for the low-density porous spheres as compared to reference UO_2 powder. The sol-gel process produces amorphous uranium trioxide and during reduction to UO_2, nano-sized crystallites are formed. These very small grains have active surfaces for sintering such that the onset temperature for sintering is lower for the sol-gel derived particles in comparison to reference UO_2.

4.1.5 Processing of Low Loss Feedstock

E. Luther, LANL

Techniques that improve the performance of uranium oxide fuel pellets or simplify the powder processing methods used to fabricate pellets are of interest to the commercial nuclear fuel industry. Low loss feedstocks have been synthesized at ORNL by the MDD (Modified Direct Denitration) process. The feedstocks are termed “low loss” because of their potential to eliminate processing steps that would

normally result in material lost in process due to hang up in processing equipment. Previously, MDD powders were studied to characterize their physical properties and obtain preliminary data on sintering behavior.

In FY2012, a variety of powder processing techniques were studied to optimize the pellet fabrication process of two compositions, pure UO_2 and 95/5 UO_2/CeO_2. It was found that the as-pressed (green) density of the MDD powders could be increased significantly by employing the powder conditioning steps of milling, sieving and addition of a pressing aid EBS (Ethylene Bis Stearamide). Figure 14 and Figure 15 show the microstructure of uranium oxide pellets prepared by optimal and less than optimal conditions resulting in sintered theoretical densities of 92% and 89% respectively.

This study demonstrated the importance of the feedstock on final properties of pellets. Although significant improvements can be made by appropriate powder conditioning techniques, issues such as powder agglomeration and morphology that degrade particle packing can be difficult to overcome resulting in pellets with less than desirable final densities.

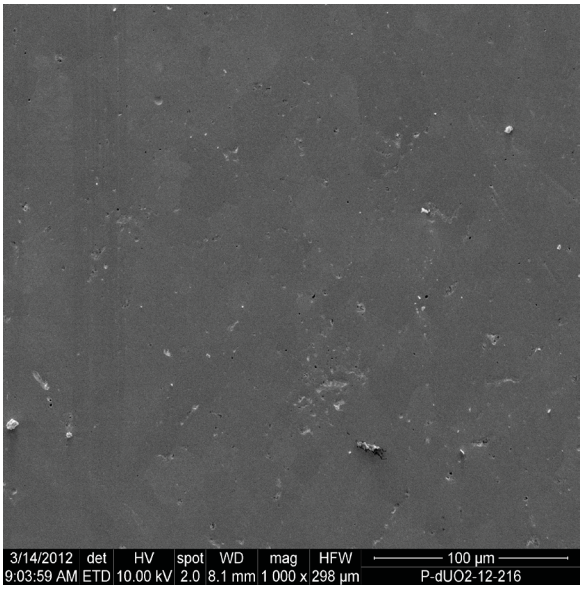

Figure 14. Pellet prepared from MDD UO_2 powder reduced at 650˚C with 0.25 wt% EBS sintered at 1650˚C for 4 hrs.

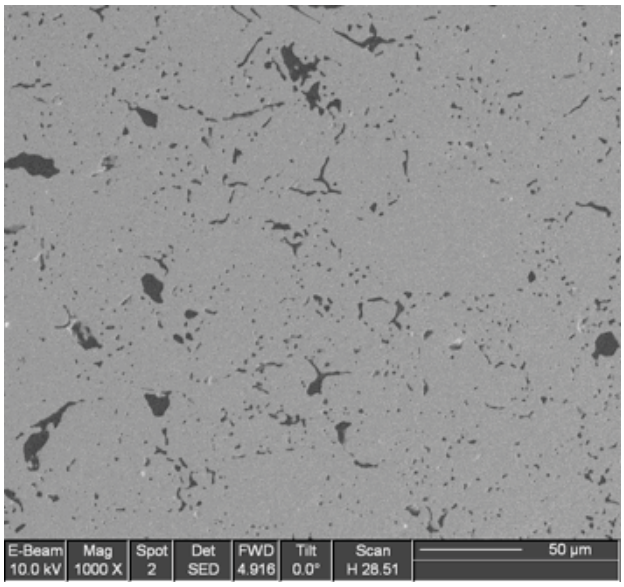

Figure 15. Pellet prepared from MDD UO_2 powder reduced at 650˚C with 0.6wt% EBS sintered at 1550˚C for 4 hrs.

4.2 Property Determination and Advanced Characterization

4.2.1 Framework for Thermokinetic Model of Oxidation of LWR UO_2 Fuel

S. Voit, ORNL

Off-normal situations may expose LWR UO_2 fuel to changing conditions that can affect the fuel-clad chemistry and accelerate chemical kinetics for reactions. These irregular events can occur in-pile, with the development of a pinhole in the clad (leaker) or loss of clad integrity during a Loss Of Coolant Accident (LOCA), or during storage of used fuel with a breach of containment (either poolside or above ground in dry interim storage).

The goal of this work is to establish a comprehensive mechanistic model of UO_2 oxidation and an engineering-scale model that can be used to predict fuel oxidation behavior under reactor off-normal events. A series of models were defined leading to the development of a mechanistically-based, engineering-scale model that will predict the molar fluxes of gas constituents in a breached fuel pin,

calculate the local time-dependent water vapor to hydrogen ratio and oxygen potential, and predict the adsorption reaction rates and subsequent oxidation kinetics of UO_2 and Zircaloy surfaces. The model will be developed using a mechanistic approach to characterize reaction and transport processes (Figure 16) under relevant conditions including exposure to partial pressures of oxygen and water at elevated temperatures.

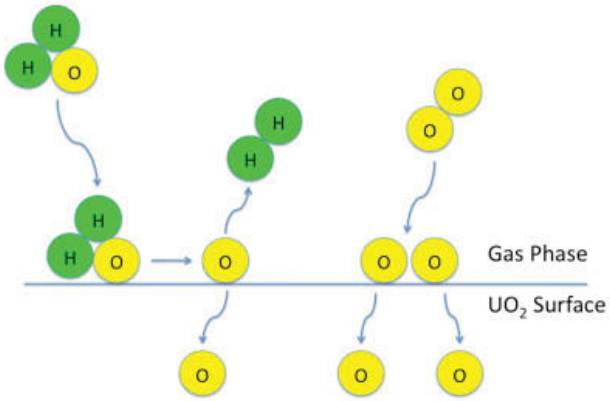

Figure 16. Adsorption on the surface and oxygen diffusion in bulk UO_2.

4.2.2 Microstructural Characteristics of Sintered Urania

K. Rudman, K. Krishnan, H. Lim, P. Peralta, ASU

Microstructure of oxide fuels plays a significant role on their performance, since it can affect transport properties and microstructure evolution in-pile. Therefore, characterization of initial microstructure can be extremely helpful to understand and model oxide fuel performance. In particular, the distribution of grain boundaries (GBs) given their crystallography is needed to understand fission product (FP) mobility, since mass transport along GBs has a strong dependence on GB character. Nonetheless, data on full GB crystallography of oxide fuels are scarce, as it requires full 3-D characterization. The aim of this study was to characterize the microstructure of oxide fuels to inform mesoscale models of FP transport.

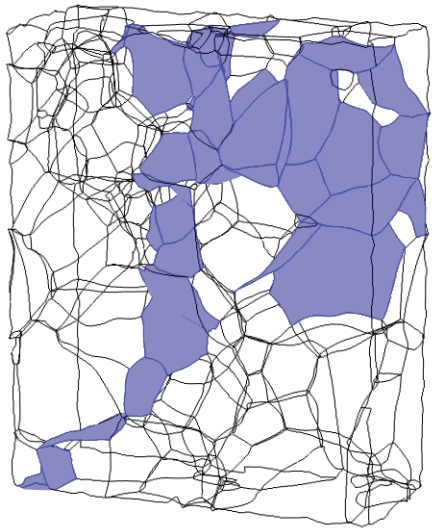

Figure 17. Skeletonized 3-D microstructure showing the GB percolation path.

Electron microscopy techniques were used to quantify the microstructure of depleted uranium oxide (d-UO_2) as a surrogate. The collected data were used to obtain statistics of GB characteristics, including misorientations and GB planes, as well as correlations between GB crystallography and the size of intergranular pores. The results were then used to study the effect of microstructure on the diffusion of FPs using finite element techniques (Figure 17).

PRESENTATIONS AND PUBLICATIONS:

[1]. H. Lim, K. Rudman, K. Krishnan, R. McDonald, P. Dickerson, D. Byler, P. Peralta, C. Stanek, K. McClellan, “Microstructurally Explicit Simulation of Intergranular Mass Transport in Oxide Nuclear Fuels.” Accepted for publication, J. Nuclear Technology, 2012.

[2]. K. Rudman, P. Dickerson, D. Byler, R. McDonald, H. Lim, P. Peralta, C. Stanek, K. McClellan. “3-D Characterization of Sintered UO2+x: Effects of Oxygen Content on Microstructure and its Evolution.” Submitted for publication, J. Nuclear Technology, 2012.

[3]. R. McDonald, K. Rudman, E. Luther, P. Peralta, C. Stanek, K. McClellan. "Porosity Characterization of Surrogates for Oxide Nuclear Fuels: A Statistical Analysis of Correlations among Grain Boundary Misorientation and Pore Character and Location." TMS Annual Meeting, Orlando, FL 2012. Poster presentation. R. McDonald won the DOE's Innovations in Fuel Cycle Research Award Competition for Students Who Attend Universities with Less than $630 Million in 2009 R&D Expenditures.

4.2.3 Experimental Characterization of LWR Fuel Performance during Off-Normal Events

A.T. Nelson, LANL

In the event of cladding failure in commercial reactors due to either a manufacturing defect or transient, fuel is exposed directly to water or water vapor at high temperatures. Pursuit of a more comprehensive understanding of how light water reactor (LWR) fuel responds to the thermochemistry of a cladding breach is therefore essential to improve existing models of off-normal performance, better predict long term storage characteristics, and design LWR fuel forms possessing superior properties under oxidizing environments.

An experimental capability to measure the oxidation kinetics of LWR fuels under water vapor atmospheres at high temperatures was established within the FCRD-AFC program during FY2012. The baseline response of UO_2 to these accident-relevant conditions was chronicled in collaboration with companion studies being performed at JAEA-Tokai under a bilateral agreement.

Typical oxidation curves are shown in Figure 18 with oxidation rates varying depending upon temperature. The different oxidation rates are attributed to changes in the phase stability as a function of temperature. As the temperature increases, the intermediate oxides present in the O-U system, namely U_4O_9 and U_3O_7, gain or lose stability. Understanding in detail how this interplay unfolds during the oxidation of UO_2 could provide key advances in development of evolutionary forms of UO_2 more resistant to degradation during a clad breach.

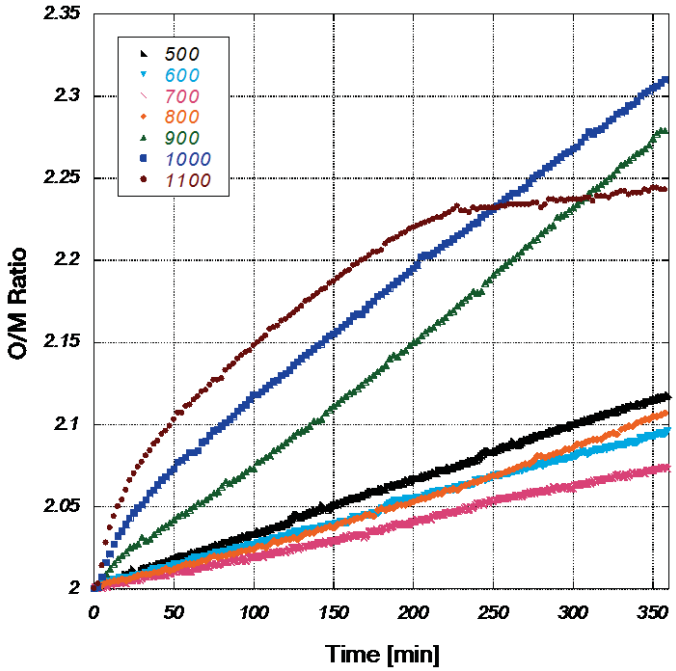

Figure 18. Oxidation of UO_2 samples in a flowing atmosphere of 25% water vapor carried in ultra high purity nitrogen. Three different regimes of oxidation behavior are seen.

During an LWR cladding failure, appreciable hydrogen is produced during oxidation of Zircaloy cladding in water vapor. This hydrogen greatly blunts the oxidation rate of UO_2. As numerous routes to

drastically minimize oxidation of cladding materials are currently under consideration, it is essential to capture the effect that such modifications to the fuel-clad system will have on the rate of fuel degradation during a potential cladding breach.

4.3 Fuel Performance and Separate Effects Testing

4.3.1 Fabrication of Ceramic Fuel Samples for Separate Effects Testing of Thermal Conductivity Degradation under Irradiation using HFIR

A.T. Nelson, LANL

The development of irradiation studies to compliment ongoing investigations of uranium dioxide (UO_2) ceramic nuclear fuels is a critical component within the SET approach to isolate and understand the influence of specific actors on all aspects of nuclear fuel operation. These studies are especially relevant to ongoing modeling efforts, as developers of predictive codes capable of capturing the numerous dynamic responses of nuclear fuels to irradiation must seek to include the highest degree of detail in the experimental data they aspire to match.

Of the numerous properties and aspects of fuel performance identified within the Ceramic Fuels Campaign Separate Effects Test Plan developed during FY2010 and FY2011, thermal conductivity is the singular area that currently receives significant attention from fuel vendors and plant operators as well as the modeling community. Preparations began in FY2011 continued into FY2012 to perform the first in a series of rabbit irradiations of oxides designed to elucidate the effect of irradiation damage on degradation of thermal conductivity in pile. A range of compositions was successfully synthesized at LANL (Table 6) under controlled conditions to prepare a series of test compositions that vary only in two key facets: feedstock synthesis route and secondary cation content. Sample preparation was performed under a controlled fabrication plan developed at LANL and executed to the rigor required for reactor test irradiations. Pre-irradiation characterization of chemistry, microstructure and thermal conductivity was also completed. Depleted uranium was used to eliminate fissions from clouding the defect generation mechanisms; future studies executed following the completion of this test will incorporate enrichment to investigate the potential role of fission product track damage on response.

Table 6. Baseline sample set for rabbit irradiation campaign to study the impact of low doses on thermal transport in ceramic nuclear fuels. Traditional ceramic solid solution (SS) processing, co-precipitation (CP), and modified direct denitration (MDD) samples are noted. All compositions are nominal atomic percentages.

Traditional Compositions	MDD Compositions
AREVA UO_2	MDD UO_2
95/5 SS UO_2/CeO_2	95/5 MDD UO_2/CeO_2
80/20 SS UO_2/CeO_2	80/20 MDD UO_2/CeO_2
95/5 CP UO_2/CeO_2	95/5 MDD UO_2/Nd_2O_3
80/20 CP UO_2/CeO_2	80/20 MDD UO_2/ Nd_2O_3

4.4 Reference Material and Technique Development

4.4.1 Oxide Thermochemical Modeling

S. Voit, B. Slone, J. McMurray, D. Shin, T. Besmann, ORNL

The thermochemical behavior of oxide nuclear fuel and targets under irradiation is dependent on the oxygen to metal ratio (O/M). When fuel is irradiated, fission fragments and free oxygen are created resulting in an average increase in O/M with fuel burnup. Some of the fission products form species that will migrate to and react with the cladding surface in a phenomenon known as Fuel Clad Chemical

Interaction (FCCI) so it is desirable to understand oxide thermochemistry in order to guide the design and fabrication of higher burn up fuel.

A phased oxide fuel thermochemical model development effort is. First, models of binary oxide systems, such as U-O, Ln-O, etc., are developed. Next, the binary systems are combined to form pseudo binary systems such as U-Ln-O. The model development effort requires the use of data to allow optimization based on known thermochemical parameters as a function of composition and temperature. Available data are mined from the literature and supplemented by experimental work as needed.

Thermodynamic data were collected for the U-Ce-O (Figure 19), U-La-O, and U-Nd-O systems to support modeling efforts for fuel fabrication and understanding of in-reactor behavior. These data were added to a consistent set of data from the literature, and the data set was then used to optimize interaction parameters within the respective compound energy formalism thermochemical models.

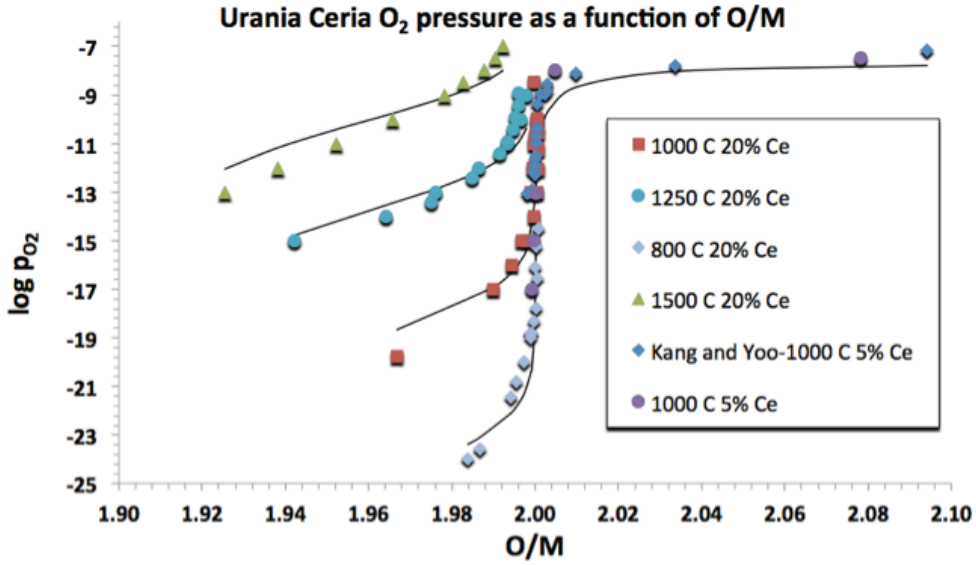

Figure 19. Plot of experimental and computed log of oxygen pressure versus O/M in the U-Ce-O system.

4.4.2 Uranium dioxide films with embedded xenon

I.O. Usov, LANL

Experimental data concerning description of Xe diffusion in UO_2 –based nuclear fuels have a wide range of disparity such that it is difficult to verify modeling results for development of predictive nuclear fuel performance codes. The goal of this work was to fabricate and characterize reference samples to isolate and quantify the inherent transport properties of Xe in UO_2. We utilized ion beam assisted deposition (IBAD) to fabricate depleted UO_2 films with embedded Xe atoms (UO_2<Xe>) [1].

In FY2012, we focused on further development of the IBAD method and determination of intrinsic parameters governing Xe behavior in UO_2 [2]. Figure 20 shows scanning transmission electron microscopy (STEM) image obtained from the annealed UO_2<1.46 at. % Xe> film. Before annealing, the sample contains large density of Xe-bubbles with an average diameter ~ 6 nm. After annealing, the bubble density is reduced dramatically and the average diameter increased up to ~ 20 nm. The diffusion coefficient of Xe atoms (D_{Xe}) can be readily estimated from the change of the average Xe-bubble diameter. The D_{Xe} value at 1000°C was estimated to be $4.7 \times 10^{-16} cm^2$.

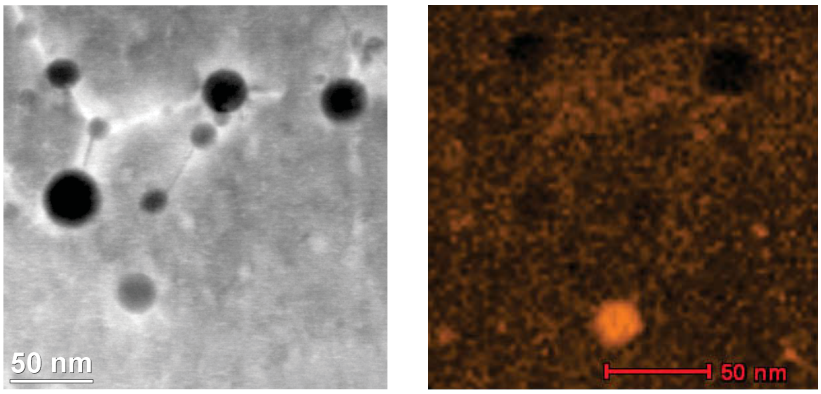

Figure 20. STEM and Xe atomic distribution measured by EDXS obtained from UO_2 film synthesized by the IBAD method and subsequently annealed at 1000 ^oC for 3 hours. The orange spherical feature represents a Xe-filled bubble.

The value of such synthetic UO_2<Xe> samples is that fission gas introduction is separated from the various effects attendant to the fission process. Our new technique offers the opportunity to develop a radiation-free, composition-controlled, systematic approach to elucidating the underlying physics of gas behavior in nuclear materials. Quantitative description of fission gas atom migration in the unperturbed UO_2 lattice is a basis for any theoretical model predicting performance of a nuclear fuel element. The findings of our investigations illustrate a great potential of the IBAD technique and UO_2 films for various areas of nuclear materials studies.

PUBLICATIONS:

[1]. I.O. Usov, J.Won, D.J. Devlin, Y.-B. Jiang, J.A. Valdez, K.E. Sickafus, J. Nucl. Mater. 408 (2011) 205.

[2]. I.O. Usov, R.M. Dickerson, P.O. Dickerson, M.E. Hawley, D.D. Byler, K.J. McClellan, submitted to J. Nucl. Mater.

4.4.3 Melt Point as a Function of Composition for Urania-Based Systems

D.D. Byler, J.A. Valdez, LANL

Due to the interest in the development of nuclear fuels which can safely handle higher/deeper burn-ups, it is critical to understand how fission product evolution, oxygen-to-metal ratios (O/M), and changes in composition affect the melting point of fuel constituents. By understanding the materials melting behavior, safety factors can be engineered into the design of fuels as well the establishment of safe operational limits. Additionally, accurate melt point values for nuclear fuels (both pristine and burned) are of extreme importance to modeling and simulation efforts in order to assess the accuracy of predictive.

In FY2012 development, the thermal arrest melt point determination systems was validated and preliminary melt point measurements of $UO_{2.00}$, urania-ceria and urania-neodymia solid solutions were completed. The measurements used an induction heating system to heat a tungsten capsule containing the sample past the melting point while recording the temperature as a function of time. To validate and test our system, we performed melt point measurements on, Niobium (Nb), Molybdenum (Mo) and on Hafnium dioxide (HfO_2) standards. The measured values agreed well with results from published data. Urania, urania-ceria and urania-neodymia melt point measurements were also successfully made (Figure 21). It can be seen from the figures that thermal arrests (material melting point) are well defined allowing determination of a materials melting point with a high degree of certainty.

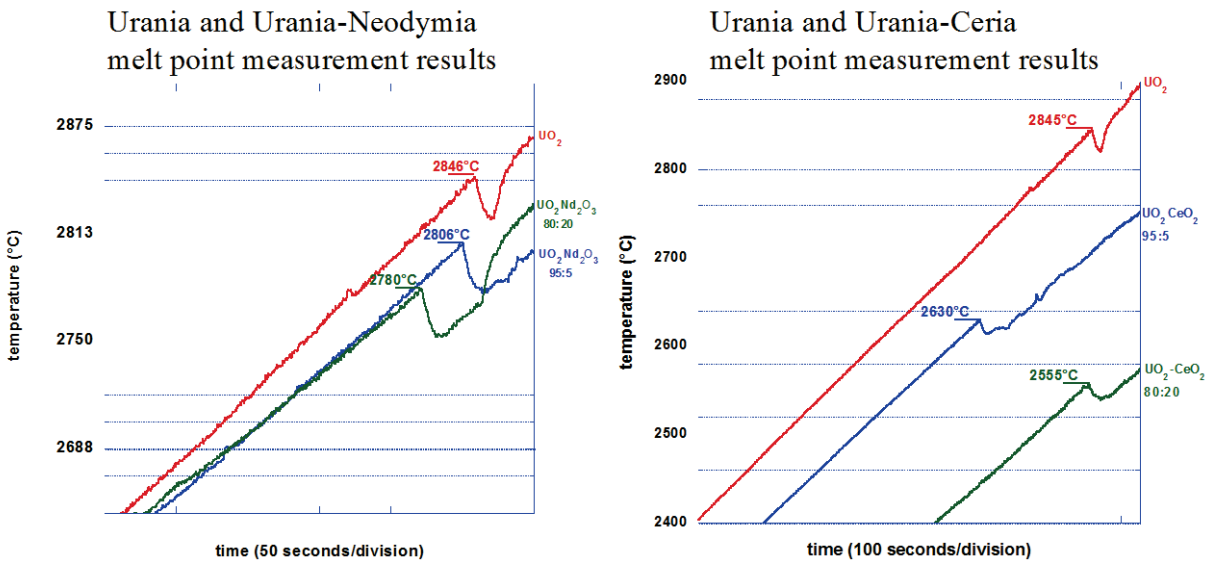

Figure 21. Thermal arrest plots showing temperature versus time. The melting point of several stoichiometric compositions in the U-Nd-O and U-Ce-O systems is shown.

4.4.4 UO_2 Crystal Growth

D.D. Byler, J.A. Valdez, K.J. McClellan, LANL

Inherent in the SET approach to coupling modeling and experiment for development of predictive fuel performance codes is the need to isolate key characteristics of microstructure such as grain boundaries. The use of single crystals provides materials that are free from grain boundary considerations and the use of large multi-crystalline materials allows the characterization of grain boundary interfaces associated with particular grain misorientations to improve predictive models. In order to enable support the SET approach crystal growth of oxide fuels is being performed.

In FY2012, several different technique assessments were continued to determine the best method to produce a set of high quality urania single crystals. Of these techniques, a solid-state technique described as exaggerated grain growth was performed because of the relative ease and lower temperature requirements to achieve a single crystal. Figure 22a illustrates a typical pellet formed by this technique and Figure 22b shows a cross-section of that pellet and the section that was harvested from it to produce a 1.5 x 1.5 x 4.5mm oriented sample used for indentation testing.

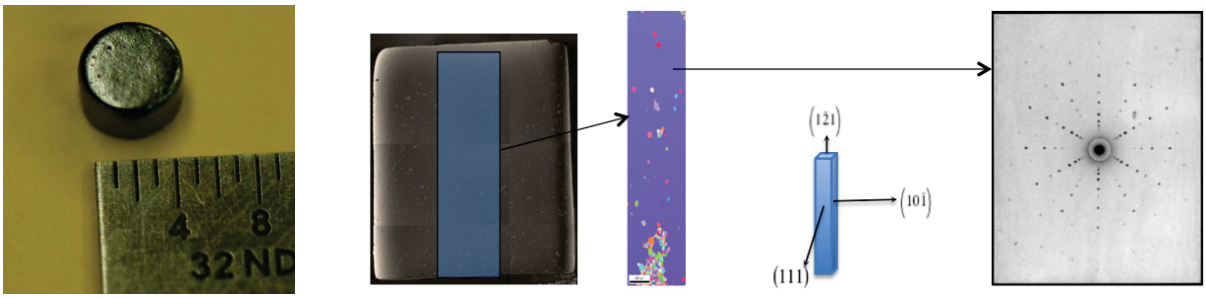

(a) (b)

Figure 22. (a) Picture of a single crystal pellet grown by the exaggerated grain growth technique, (b) cross-section of pellet illustrating the area harvested for a single crystal, an EBSD image and the x-ray back reflection Laue pattern of the harvested sample.

Additionally, growths from the melt were performed using the Bridgman technique. Crystals or very large grains were produced up to ~5mm in size, with very low or no porosity present. Based on this technique, larger high quality crystals of varying compositions can be grown for use as reference materials and for fundamental property measurements. Several crystals have been grown and characterization of the crystals is continuing to produce a set of crystals suitable for testing as reference materials.

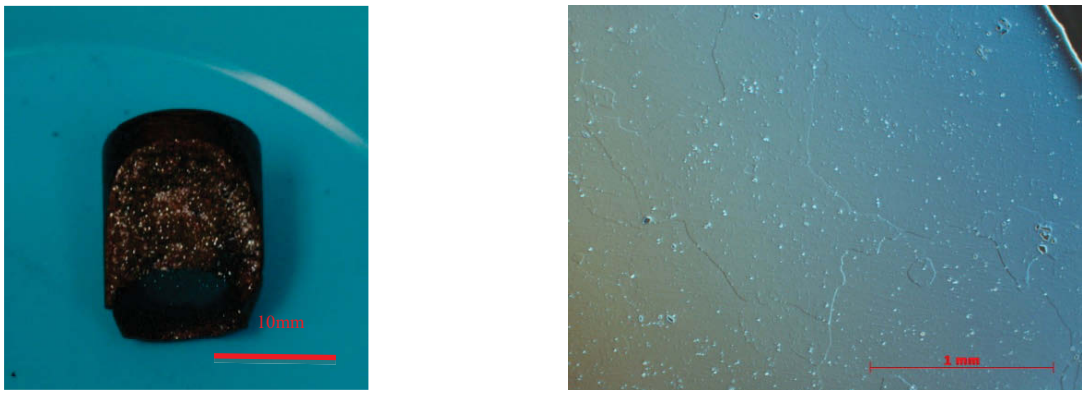

(a) (b)

Figure 23. (a) Image of cast urania from Bridgman growth technique and (b) microstructure of cross-section of this cast segment of urania.

In summary, two crystal growth techniques were developed with the Bridgman technique producing the best overall crystal with the highest density. Urania crystals have been grown by both techniques and are in the process of harvesting and characterization to determine quality, orientation, O/M, etc. to be used as reference materials and for fundamental property measurements. The Bridgman technique can be scaled up to produce larger crystals for various fuels related activities and meet the needs of the fuels community. The exaggerated grain growth technique has the unique capability to produce very large single crystals for use as reference samples with the proper growth conditions, although embedded porosity is a continuing issue that must be addressed with this technique.

5. MICROENCAPSULATED FUELS TECHNOLOGIES

L. Snead, sneadll@ornl.gov, ORNL

Coated Particle Fuels Technologies focused on the application of coated particle fuel technology for advanced reactor platforms including LWR applications. It is highly integrated with direct modeling, fuel fabrication, irradiation testing, and post irradiation performance evaluation. FY 2012 focus areas included modeling, TRU TRISO Development, LWR Microencapsulated fuel development, and the testing of advanced clad and fuel materials being developed for enhanced safety under FCRD and other programs.

5.1 Compatibility/Stability Issues in the Use of Nitride Kernels in LWR TRISO Fuel

T. M. Besmann, B. L. Armstrong, ORNL

The use of UN fuel kernels for LWR TRISO fuel raises concern that the SiC layer may be nitrided by nitrogen from the fuel and thereby lose its effectiveness as a pressure and fission product barrier. Specifically, the concerns relate to free nitrogen produced during fission attacking the SiC layer. This would possibly jeopardize the stability of the SiC layer with the potential conversion into Si_3N_4 or Si(C,N).

The stability of the SiC layer in the presence of free nitrogen may be dependent upon the operating temperatures. Under accident scenarios, due to the high FCM thermal conductivity in comparison to UO_2, the fuel temperature will be at most 100-200°C above the 1200°C loss of coolant accident (LOCA) condition, and then for only a limited period of time. Although nitrogen released in fissioning will form fission product nitrides, there will remain an overpressure of nitrogen of some magnitude. The nitrogen can be speculated to transport through the inner pyrolytic carbon layer and contact the SiC layer. The SiC layer may be envisioned to fail due to resulting nitridation at the elevated temperatures. However, it is believed that these issues are particularly avoided in the LWR application. Lower temperatures will result in significantly lower nitrogen pressures. Lower temperatures will also substantially reduce nitrogen diffusion rates through the layers and nitriding kinetics. Kinetics calculations were performed using an expression for nitriding silicon. In order to further address these concerns, experiments were run with surrogate fuel particles under simulated operating conditions to determine the resulting phase formation at 700 and 1400°C.

A review of the literature revealed very limited publications on nitriding of SiC. There is, however, considerable literature on nitriding of silicon, mostly for producing silicon nitride components. For purposes of assessing the issue of nitriding SiC in a TRISO particle the use of relations for nitriding silicon would be a conservative assumption as elemental silicon would be more reactive. The intrinsic kinetics expression of Maalmi and Varma[1] for nitriding silicon powder was used to obtain a very conservative assessment and yielded Figure 24.

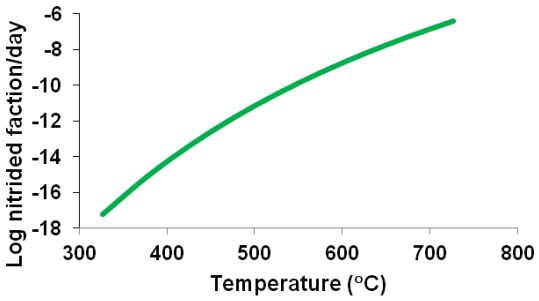

Figure 24. Fraction of a 35 µm SiC layer nitrided per day in reactor as a function of fuel temperature computed from the relations of Maalmi and Varma.[a]

An experimental verification of the expected slow kinetics for nitriding SiC under LWR FCM conditions was performed using SiC coated surrogate TRISO particles, i.e., particles without the outer pyrolytic carbon layer. These were exposed at 700°C in a 1 atm. gas environment with flowing 60

[a] M. Maalmi and A. Varma, AIChE Journal, **42** *12* (1996) 3477

ccm argon with a balance of 4% hydrogen plus 240 ccm of ultra high purity (UHP) nitrogen for 168 h. Higher temperature exposures at 1400°C were made for 24 h. An example of the results is seen in Figure 25.

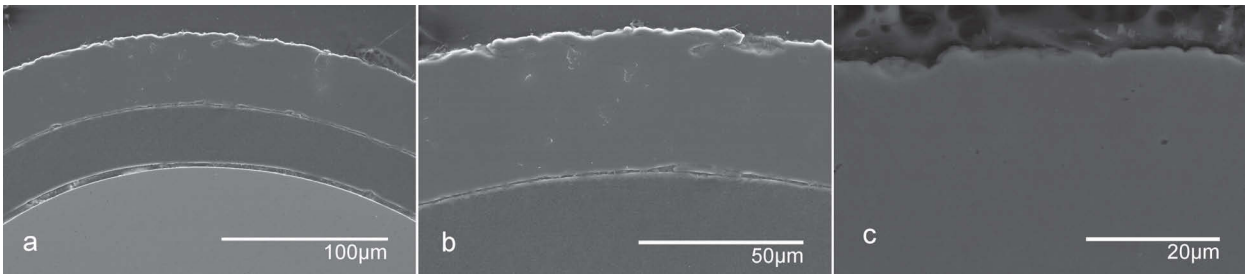

Figure 25. Scanning electron microscopy images of SiC exposed to nitriding conditions at 1400°C for 24h.

Calculations based on very conservative assumptions and a set of experiments all indicate that under LWR FCM fuel operating conditions and limited period high temperature accident conditions the nitriding of the TRISO SiC layer is not an issue. The limited experimental results confirm this conclusion.

5.2 Uranium Nitride as LWR TRISO Fuel: Thermodynamic Modeling of U-C-N

T. M. Besmann, D. Shin, T. B. Lindemer, ORNL

The preparation of UN by the carbothermic reduction of urania followed by nitriding, and the intimate contact of a UN TRISO kernel with the carbon of the buffer layer is the reason for the current interest in the U-C-N system. The reported measurements with respect to U(C,N) were reviewed and used in a study to determine a solid solution representation of the phase. The model for the phase, together with free energies for the elemental and binary phases, was in turn used to derive high temperature ternary U-C-N phase diagrams. Equilibrium nitrogen pressures have been computed for conditions of interest for fabrication and in-reactor behavior of U(C,N) LWR TRISO fuel.

The reported values of the free energy expression for UN all yield calculated nitrogen decomposition pressures that are significantly lower than almost all reported measurements. Figure 26 illustrates the disagreement between computed and measured values. This discrepancy also extends to measurements of nitrogen decomposition pressures measured over U(C,N) when an ideal solution model is used to represent the phase, as detailed below. An effort was thus made to adjust the thermodynamic values for UN to obtain better agreement with nitrogen pressure data. (Note that considering the non-stoichiometry of UN would increase the discrepancy as hypostoichiometric UN would be computed to have an even lower nitrogen decomposition pressure.) The adjustment of the UN Gibbs free energy by +12 kJ/mol from the reported values yields an equivalent 298K heat of formation of -282.3526 kJ/mol, which brings the computed pressures into relative agreement with reported measurements (Figure 26), and the resultant free energy values for UN were used in representing U(C,N).

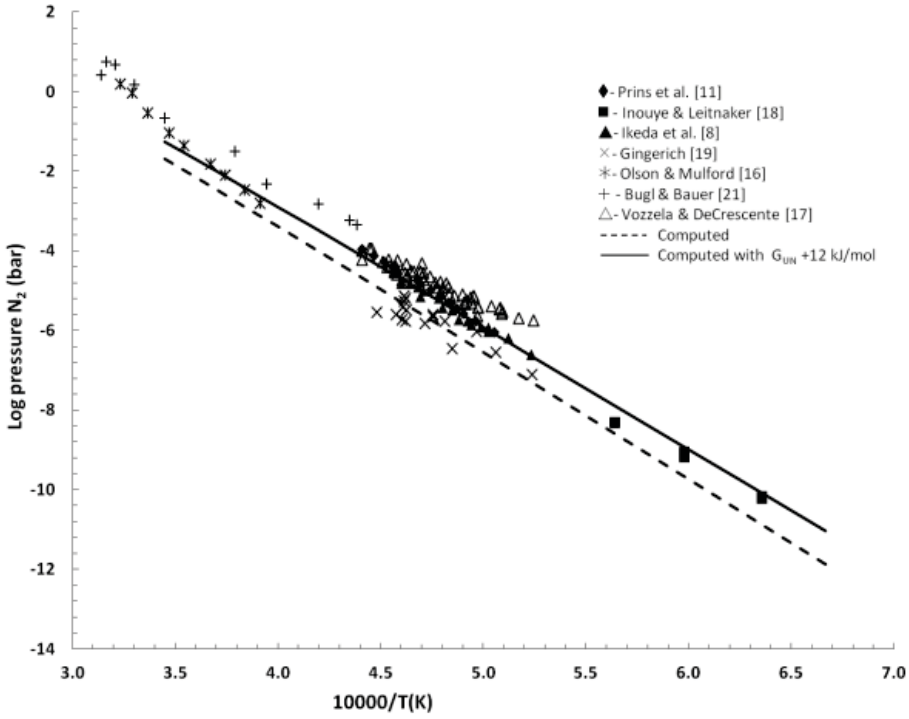

Figure 26. Plot of reported UN decomposition nitrogen pressure versus reciprocal temperature data and computed pressures.

A model for the U(C,N) phase was generated by assuming an ideal solution between the UC and UN phases. With the adjustment noted above, and concomitant adjustment to the free energy of the U_2N_3 phase, it is possible to reproduce the phase diagram for the system as best as it is understood (example in Figure 27). The model also allows computing of nitrogen pressures as a function of temperature and composition within the various phase fields, an example of which is seen in Figure 28. The ability to provide predictive phase equilibria and chemical activities will be important in supporting fuel processing and in-reactor behavior.

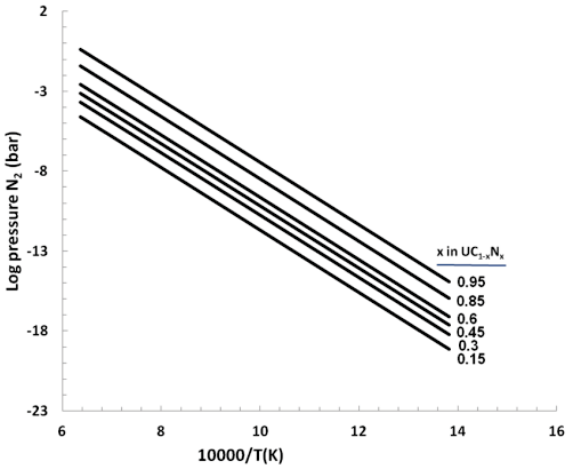

Figure 27. Computed U-C-N phase diagram at 1500K and 1 bar total.

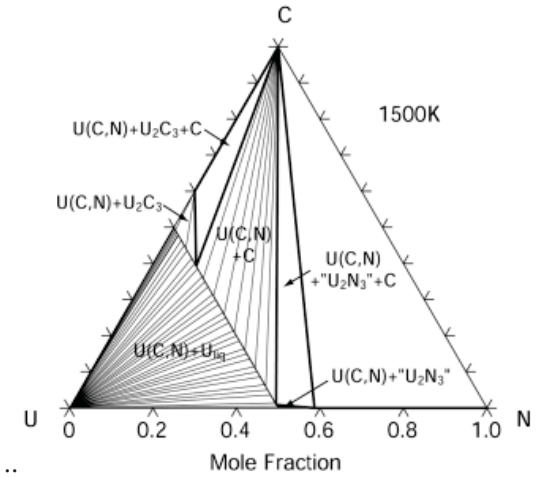

Figure 28. Computed nitrogen pressure as a function of temperature over 723K-1573K and UC1-xNx composition in equilibrium with carbon or carbides.

5.3 Severe Accident Test Station Deployment

B.A. Pint, J.R. Keiser, K.A. Terrani, L.L. Snead, ORNL

The first furnace of the severe accident test station (SATS) was successfully deployed in FY-12 capable of 1700°C in flowing steam. This effort is part of an ongoing plan to repatriate LOCA testing of irradiated fuels and to extend this testing into the Beyond LOCA performance regime. The FY-12 deliverable was the design and construction of the high-temperature (severe accident test furnace, or beyond LOCA furnace) and the initial design for installation into the 3525 hot cell at ORNL. The severe accident test module consists of a steam generator connected to two $MoSi_2$ furnaces installed in series. One furnace serves as the pre-heater and the second as the test article furnace where the article is exposed to high-temperature steam (Figure 29). The tests are performed inside an alumina (or sapphire) test tube with 100% steam or steam-H_2 gas mixtures. So far the steam flux during the tests has been set at 7 mg/cm^2-s (corresponding to 60 cm/sec flow velocity inside the test tube at 1600°C). Meanwhile, flow rates well below and above this value are readily achievable. The maximum test temperature demonstrated to date with 100% steam flow inside the furnace is 1700°C, 100°C in excess of the target temperature. The system underwent initial testing on samples of nickel aluminide and silicon carbide to 1700°C with flawless performance. The system is fully automatic and is controlled via a computer and instrumentation cabinet. Operation of furnace and gas delivery system is all performed remotely. Care has been taken to avoid use of electronic components on the gas delivery system and instead use pneumatic systems that enable higher reliability in the hot-cell environment. The plans for the upcoming year are to use this existing capability for screening of advanced materials while building an identical facility for insertion into the 3525 hot cell. In parallel, the lower temperature "quench" furnace capable of NRC-compliant LOCA testing will be designed and built.

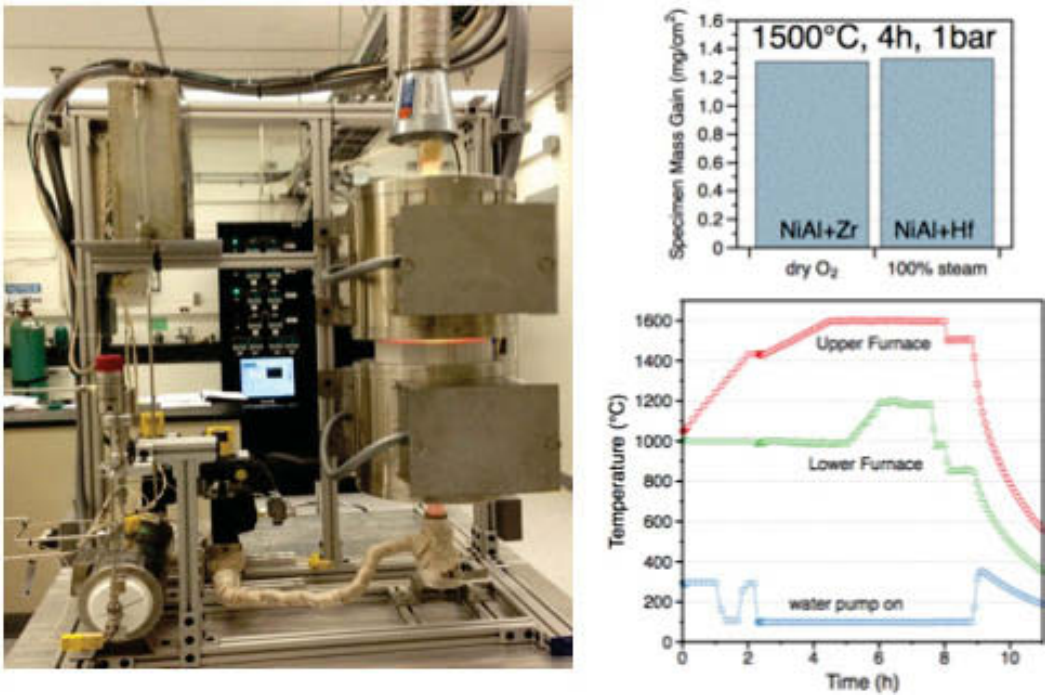

Figure 29. High-temperature furnace module of the SATS during operation.

6. CORE MATERIALS TECHNOLOGIES

S. Maloy, maloy@lanl.gov, LANL

Core Materials Technologies focused on fast reactor clad materials for high dose applications and advanced LWR clad for enhanced accident tolerance in the following R&D areas: Knowledge base development for - High Dose (up to 200 dpa) Core Materials Irradiation Data (ACO-3 duct testing and FFTF/MOTA testing) and Advanced Material Development (advanced cladding materials and coatings/liners to mitigate FCCI).

6.1 High Dose Testing of Oxide Dispersion Strengthened Steels for FR Cladding Applications

M. Toloczko, PNNL; P. Hosemann, UC Berkeley; S. Maloy, LANL

Oxide dispersion strengthened (ODS) ferritic alloys are candidate materials for fuel cladding in the FCRD advanced fast reactor concept because of their generally high temperature creep strength characteristics. MA957, developed during the National Clad and Duct program and irradiated to doses as high as 121 dpa in FFTF, is one of the first ODS ferritic alloys developed with fast reactor fuel cladding in-mind. A variety of examinations have started on these irradiated specimens, including tensile tests and atom probe tomography (APT) examinations of the microstructure. Tensile tests have revealed substantial increases in yield strength (YS) and ultimate tensile strength (UTS) after irradiation to as high as 103 dpa at temperatures from 412°C to as high as 750°C indicating a significant effect of irradiation (Figure 30). Surprisingly, uniform elongation which typically drops as strength increases, remained as good as or better than the unirradiated material for all but the 412°C irradiation temperature (Figure 30).

An initial scoping assessment of the microstructure using APT has revealed similar oxide and second phase structures among all the irradiated materials with the exception that irradiation at 412°C caused the formation of a second phase precipitate known as alpha prime, and this irradiation temperature may have also caused a refinement in the oxide particle population. Increases in the density of hard obstacles to dislocation motion are known to cause reductions in uniform elongation by reducing dislocation mobility. The reason, however, for increased strength at the higher irradiation temperatures while maintaining good uniform elongation is still under investigation with more APT examinations planned.

This early assessment showing an effect of irradiation on tensile properties, the formation of a second phase, and possible refinement of the oxide particle population suggests that ODS ferritics may have some similar responses to irradiation as tempered ferritic/martensitic (F/M) steels, however it is important to keep in mind that tempered F/M steels generally have quite good irradiation tolerance. Recent swelling and irradiation creep measurements on MA957 showing better response than HT-9 suggest that the advantage of ODS ferritics will potentially lie in their ability to match the mechanical performance of tempered F/M steels at low to moderate irradiation temperatures while having better swelling and high temperature irradiation creep resistance.

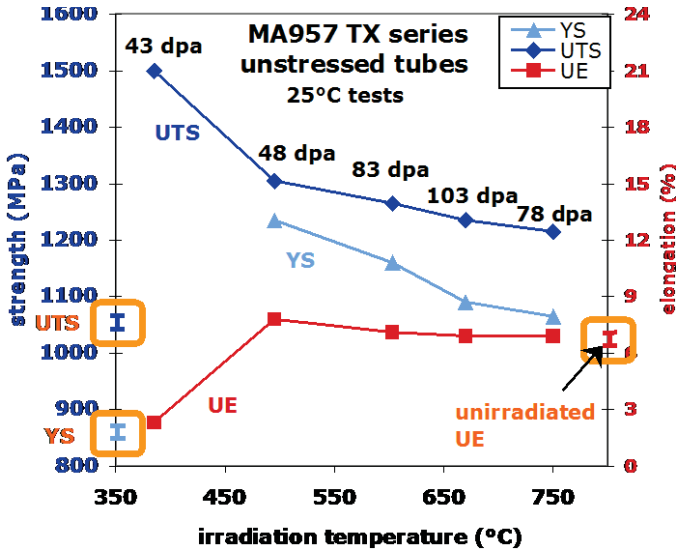

Figure 30. Tensile properties of MA957 as a function of irradiation temperature.

REFERENCES:

[1]. Toloczko, M.B., F.A. Garner, and S.A. Maloy, Irradiation creep and density changes observed in MA957 pressurized tubes irradiated to doses of 40-110 dpa at 400-750 degrees C in FFTF. Journal of nuclear materials, 2012. 428(1-3): p. 170-175

6.2 Preparing Specimens for a High Dose Irradiation in BOR-60

S. Maloy, T. Saleh, T. Romero, LANL; M. Toloczko, PNNL

Researchers at LANL and PNNL through a CRADA with Terrapower are preparing specimens of HT-9 (which were previously irradiated in FFTF to doses up to 200 dpa) for inclusion in an irradiation in BOR-60. Over 200 specimens in the shape of tensile, bend and disk specimens are being electro-discharge machined from plates cut from a HT-9 Duct (ACO3) which was previously irradiated in the FFTF. Following machining, specimens will be sent to Russia for an irradiation in BOR-60 to irradiate at the previous irradiation temperatures to doses up to greater than 400 dpa. This data will develop high dose limits for HT-9 to lead to improved radiation tolerant alloys in the future (Figure 31).

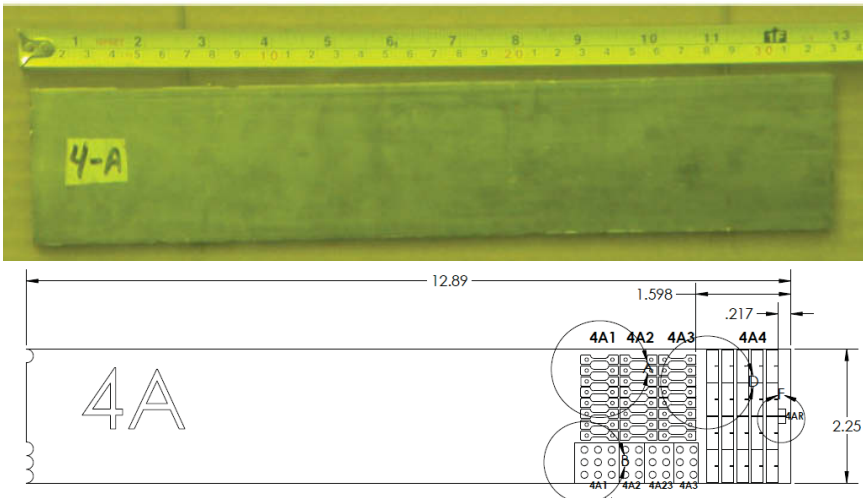

Figure 31. HT-9 Irradiated Duct Specimen

PUBLICATIONS:

[1]. O. Anderoglu, J. Van den Bosch, P. Hosemann, E. Stergar, B.H. Sencer, D. Bhattacharyya, R. Dickerson, P. Dickerson, M. Hartl, S.A. Maloy, "Phase stability of an HT-9 duct irradiated in FFTF," Journal of Nuclear Materials, Volume 430, Issues 1–3, November 2012, Pages 194–204.

6.3 Large Scale Development of 14YWT, FCRD-NFA1, for Fast Reactor Cladding Applications

S. Maloy, D. T. Hoelzer, LANL; G. R. Odette, ORNL

Researchers at LANL and ORNL in collaboration with UC Berkeley, UCSB, ATI and Zoz have completed milling of 45 kg (in 15 kg batches) of 14YWT (an advanced radiation tolerant material). A line scan shown in Figure 32 displays a uniform distribution of Y and Ti measured through the powder which shows that uniform milling that was observed in this large scale milling run. This is a first step towards large scale development of this alloy for nuclear applications. Initial testing of fracture toughness at low temperatures, creep strength at high temperatures and tensile properties look very promising. Future processing studies will include producing sheet and thin walled tubing from this alloy. Although this alloy shows most promise for fast reactor application, similar alloys with increased aluminum content (for oxidation resistance) may have applications in LWR cladding applications.

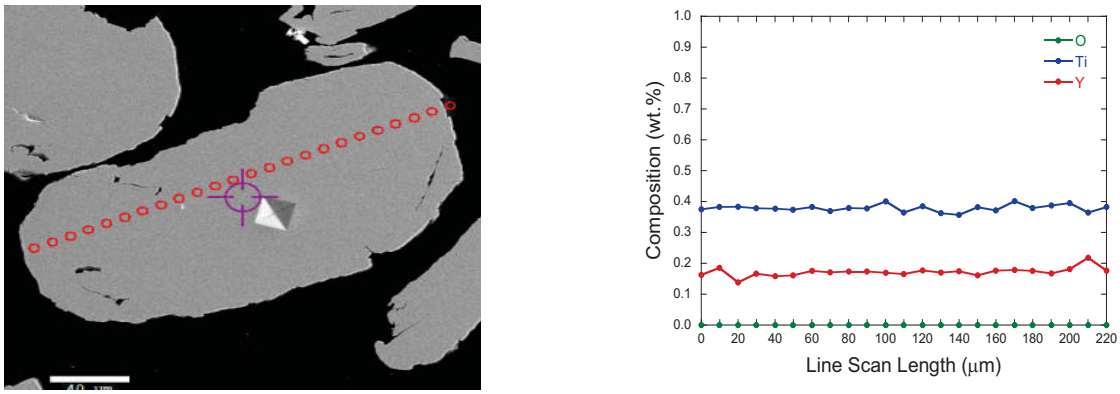

(a) (b)

Figure 32. A SEM micrograph in (a) shows a red dotted line along which Y, O and Ti were measured and values are shown in (b).

6.4 Development of High Toughness Nanostructured Ferritic Alloys for Reactor Core Applications

T. S. Byun, D. T. Hoelzer, ORNL; J. Yoon, KAERI

The main objective of this I-NERI collaboration with KAERI, South Korea, is to develop high-toughness nanostructured ferritic alloys (Fe-9Cr based NFAs) for future reactor core applications. The proposed approach was to strengthen grain boundaries for high fracture toughness by inducing partial phase transformation and/or by activating deformation-recovery mechanisms at or near the grain boundaries. In FY 2012, the second project year, a variety of post-extrusion thermo-mechanical treatments (TMTs) have been tried in search of an optimum process for high fracture toughness. To optimize the isothermal annealing condition, specimens were annealed at intercritical temperatures (830 – 975˚C) for 30 minutes to 20 hours. Further, the controlled hot-rolling at 900 – 1000˚C for 20 or 50% thickness reduction have been applied to induce extensive deformation-recovery mechanisms. Various microstructural and mechanical characterizations: differential scanning calorimetry (DSC), in-situ high temperature XRD, nano-indentation test, high temperature tensile and in-vacuum fracture tests, have been performed for providing feedback data as well as for accumulating property data. The main goal of this

project, process development for high toughness NFAs, is believed to be well achieved as some of the post-extrusion TMTs resulted in the fracture toughness values as high as those of the bench mark materials (ferritic/martensitic steels), as displayed in Figure 33. Detailed microstructural and mechanical characterizations for optimized NFAs will be the main activities of FY2013. As a successful development of high toughness NFA is currently being assured, the next stage of research will be proposed in the final year, which may include irradiation experiment, weldability study, and fabrication in tube form.

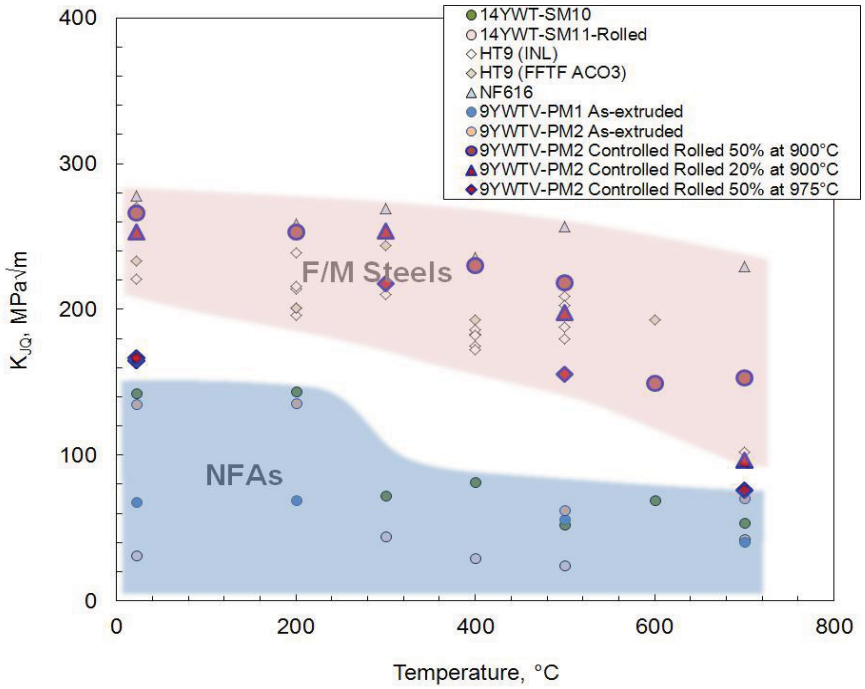

Figure 33. Temperature dependence of fracture toughness in 9YWTV-PM2 after hot-rolling at 900 and 975°C compared to those of F/M steels and other NFAs.

6.5 Cladding Coating and Liner Development for FCCI Mitigation

J. Gan, J. Cole, INL; F. Khatkhatay, J. Jian, L. Jiao, H. Wang, Texas A&M University

Researchers at INL in collaboration with The Texas A&M University produced TiN coated HT-9 cladding tubes for a future high burnup fuel irradiation experiment in ATR. The program successfully demonstrated the effectiveness of a thin layer 500-1000 nm thick TiN coating on suppressing the Fe-Ce interaction from annealing in a vacuum furnace. The back scattered SEM images show the cross section of a diffusion couple with (middle) and without (right) a TiN coating layer between Ce and Fe after annealing at 550°C for 48 hours. The interface with 500 nm TiN shows no interaction while the interface without TiN coating shows an interaction zone of approximately 30 µm. A journal article on TiN coating was published (Journal of Nuclear Materials, Vol. 429 (2012) 143-148).

A long-cladding-tube inner-wall laser deposition system capable of coating one foot (30.5 cm) long HT-9 cladding for future high burnup fuel irradiation test in ATR has been developed and installed. Three pictures on the left show the general view (top) and the motor driven tube holder (middle) of the system and a glass tube (bottom) of similar dimensions to a HT-9 cladding with its inner wall coated for demonstration. Two 7-inch long HT-9 cladding tubes were successfully coated with 1-µm thick TiN diffusion barrier layer on the inner wall as shown in the picture (Figure 34). These coated cladding tubes will be used for high burnup fuel irradiation test in the ATR.

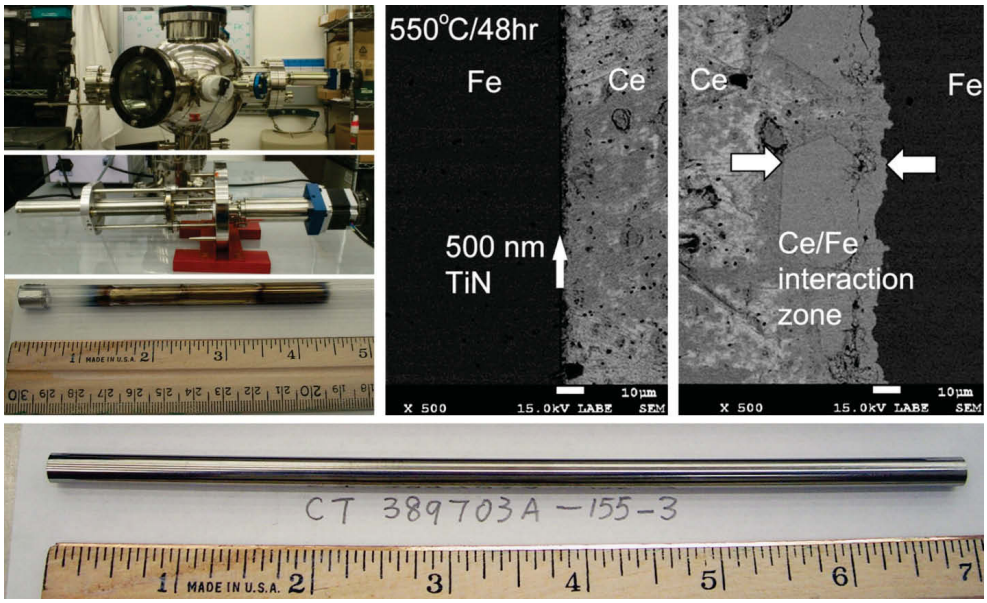

Figure 34. Cross-section of a diffusion couple with (middle) and without (right) a TiN coating layer between Ce and Fe after annealing at 550°C for 48 hours.

6.6 ORNL High-Pressure Steam Tests

B.A. Pint, J.R. Keiser, K.A. Terrani, L.L. Snead, ORNL

Oxidation tests in 100% steam and 50% steam-50% H_2 environments were performed at ORNL's high pressure oxidation facility. During the tests, a wide range of candidate fuel and cladding materials were examined to inform the fuel development activities under the Fuel Cycle R&D program at DOE-NE. The tests were performed over the temperature range of 800-1350°C for various durations up to 48 hours. Among the various iron-based alloys that were examined FeCrAl class of alloys with >20wt% Cr content and ~5 wt% Al content proved to be the most oxidation resistant. Figure 35 shows the results of 8 hour test at various temperatures where the Kanthal APMT alloy (Fe- 22Cr-5Al-3Mo) exhibits exceptional oxidation resistance.

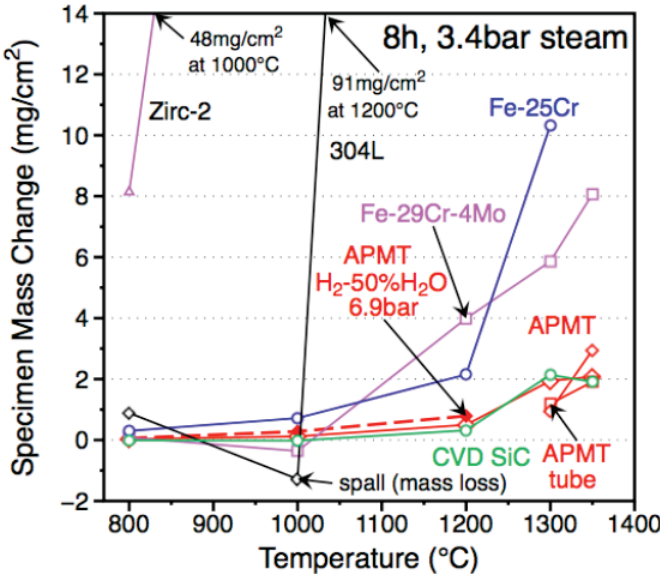

Figure 35. Specimen mass change data after exposures in 3.4 bar steam as a function of temperature for 8h exposures.

PUBLICATIONS:

[1]. B. A. Pint, M. P. Brady, J. R. Keiser , T. Cheng and K. A. Terrani, “High Temperature Oxidation of Fuel Cladding Candidate Materials in Steam-Hydrogen Environments,” Proceedings of the 8th International Symposium on High Temperature Corrosion and Protection of Materials, Les Embiez, France, May 2012, Paper#89.

7. IRRADIATION TESTING

S. Hayes, Steven.Hayes@inl.gov, INL

Irradiation Testing Technologies focused on continued irradiation of fast reactor fuel concepts in ATR, preparations for SET fuel testing using the hydraulic rabbit facility in HFIR, and postirradiation examinations of fuels irradiated in ATR, EBR-II and FFTF.

7.1 Irradiation Testing of Transmutation Fuels in ATR

K. Barrett, G. Chang, H. Chichester, S. Hayes, M. Lillo, INL

The AFC-2D and AFC-2E experiments completed irradiation in ATR and were discharged in April 2012. The AFC-2D experiment contained 6 high-burnup MOX fuel rodlets, with 4 also containing minor actinides to study transmutation fuel performance. AFC-2D is a companion experiment to AFC-2C, a low burnup MA-MOX fueled experiment whose baseline postirradiation examination was completed in 2011. The AFC-2C and 2D experiments were the first minor actinide-containing oxide fuels irradiated in the FCRD program.

The AFC-2E experiment was designed to study metallic fuel fabrication variables and provide a direct connection between current irradiation testing using a cadmium shroud to mimic fast reactor conditions in ATR vs. historic EBR-II reactor conditions. The AFC-2E experiment included archive EBR-II fuel fabricated by injection casting along with newly fabricated fuel of the same composition using arc-casting. The experiment also contained fuel with minor actinides to study transmutation fuel performance.

Postirradiation examination of both experiments will provide valuable data regarding fuel performance of both standard oxide and metallic compositions along with minor actinide-bearing fuels for transmutation. In addition, these experiments will contribute important data on fast reactor fuel behavior in a modified thermal spectrum which will be compared to historic fuel behavior in fast reactors. These results will be published in the Thermal Spectrum Testing of Fast Reactor Fuels Comparison Report.

Table 7. AFC-2D Irradiation

Rodlet	AFC-2D †	Average LHGR (W/cm)	Fission Density (f/cm^3)	$^{235}U + {}^{239}Pu$ (at.%)	HM (at.%)
1	1. $(U_{0.75},Pu_{0.2},Am_{0.03},Np_{0.02})O_{1.95}$	217	2.22 E21	24.5	13.3
2	2. $(U_{0.8},Pu_{0.2})O_{1.98}$	291	2.99 E21	32.1	16.9
3	3. $(U_{0.75},Pu_{0.2},Am_{0.03},Np_{0.02})O_{1.98}$	315	3.22 E21	34.9	19.1
4	4. $(U_{0.8},Pu_{0.2})O_{1.98}$	DUMMY Rodlet			
5	5. $(U_{0.75},Pu_{0.2},Am_{0.03},Np_{0.02})O_{1.95}$	295	3.01 E21	32.8	17.9
6	6. $(U_{0.75},Pu_{0.2},Am_{0.03},Np_{0.02})O_{1.98}$	240	1.85 E21	27.2	14.8

AFC-2D inserted cycle 143A, Sept 2008; discharged cycle 150B, Apr 2012; 633 EFPD
† Fuel composition expressed in mole fraction.

Table 8. AFC-2E Irradiation

Rodlet	AFC-2E †	Average LHGR (W/cm)	Fission Density (f/cm^3)	$^{235}U + ^{239}Pu$ (at.%)	HM (at.%)
1	U-20Pu-10Zr	319	3.08 E21	15.9	11.5
2	U-20Pu-10Zr (EBR-II)	336	3.34 E21	21.2	11.9
3	U-20Pu-3Am-2Np-10Zr	337	3.37 E21	23.2	12.6
4	U-20Pu-10Zr	364	3.53 E21	24.0	12.3
5	U-20Pu-3Am-2Np-10Zr	339	3.27 E21	21.6	12.5
6	U-20Pu-10Zr (EBR-II)	281	2.76 E21	17.7	9.9

AFC-2E inserted cycle 145A, Nov 2009; discharged cycle 150B, Apr 2012; 483 EFPD
† Alloy composition expressed in weight percent.

7.2 Hydraulic Rabbit Testing of Metallic Fuel Specimens in HFIR

G. Bell, J. McDuffee, R. Ellis, ORNL; M. Okuniewski, INL

A series of low-dose irradiations of metallic fuel specimens fabricated at the INL were performed using the HFIR Flux Trap Hydraulic Tube Facility at ORNL. Gd shielded rabbit capsules (Figure 36), designed to maximize the fast-to-thermal neutron flux ratio, containing depleted uranium (DU-8.2wt%Zr) metallic fuel specimens were inserted into the core and ejected while HFIR was operating at full power; these experiments represent the first hydraulic rabbit tests performed in HFIR with fueled rabbits. The irradiated rabbits were shipped to the INL where post irradiation examination will be performed in FY13. The purpose of these experiments is to develop a fundamental understanding of the evolution of the microstructure of metallic fuel materials as a function of elemental composition, temperature, and neutron fluence so as to better understand the in-service behavior and performance of the fuel. The low-dose irradiation performance data being generated by this work will be used to inform and validate the advanced modeling and simulation effort on nuclear fuels. Following irradiation of the fueled rabbits, a series of dosimetry rabbits were irradiated to measure the neutron fluence and capsule temperatures over the duration of the run cycle to verify the calculated values. Additional metallic fuel compositions are scheduled for irradiations to occur in FY13.

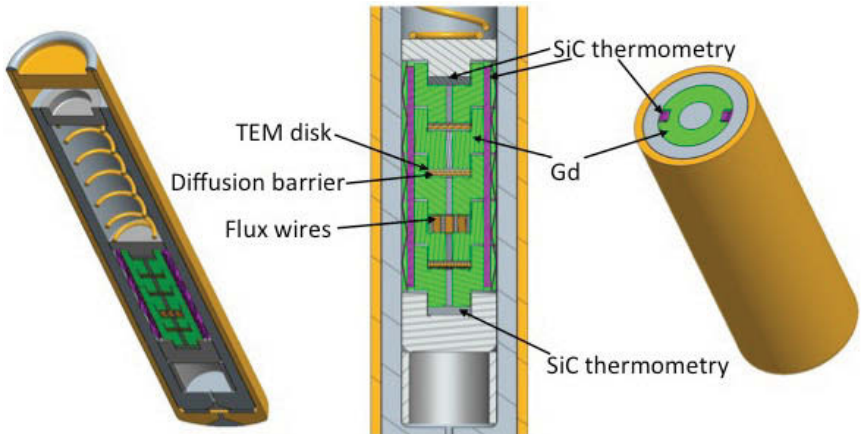

Figure 36. TEM rabbit design features the use of Gd spacers (22.86 mm stack length) that also serve as the thermal neutron shield. Space is provided for a maximum of 6 TEM disks samples. SiC temperature monitors and flux monitors displaced some of the TEM disks for the first round of experiments. The number of Gd spacers can be reduced to adjust the reactivity of the rabbit.

PUBLICATIONS:

[1]. G. L. Bell, J. L. McDuffee, R. J. Ellis, D.C Glasgow, R. G. Sitterson, L. L. Snead, and J. E. Schmidlin "Summary of FY12 HFIR Irradiation Testing Activities," ORNL/TM-2012/454, September 28, 2012.

7.3 Advanced Metallic Fuel Concept Feasibility Test in ATR

H. Chichester, R. Mariani, S. Hayes, R. Fielding, T. Hyde, T. O'Holleran, K. Barrett, G. Chang, INL; A. Wright, ANL

An advanced metallic fuel concept is being developed as a collaborative effort between Idaho National Laboratory and Argonne National Laboratory. The concept incorporates major innovations that include decreased fuel smear density, annular fuel compared to solid rod fuels, coatings or liners on inner cladding wall, vented fuel pin, advanced fabrication methods, targeted fuel alloy additions, U-Mo based fuel alloy, and compatibility with an electrochemical fuel recycling process. As part of the effort, fuel experiments to demonstrate feasibility of several key components of the concept were designed for irradiation in the Advanced Test Reactor (ATR). Eight miniature fuel pins were fabricated and inserted into ATR (Figure 37). The incorporation of palladium in the fuel alloy is intended to chemically bind the lanthanide fission products as they form, in lieu of coatings or liners on the inner cladding wall. After three cycles, the fuel pins reached approximately 2.5 to 3.5 at.-% burnup and were discharged. Postirradiation examinations of these experiments is scheduled to begin in FY13.

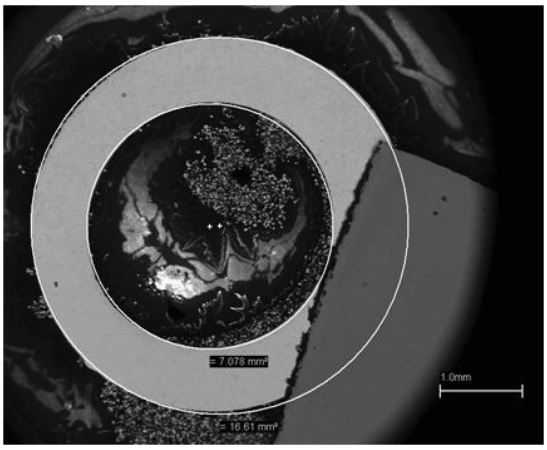

Capsule	Alloy	Geometry	Smear Density	Thermal Bond
A-1	U-10Mo	Solid	75%	Na
A-2	U-10Mo	Annular	55%	He
A-3	Materials testing for coating / liner applications			
A-4	U-10Zr	Annular	55%	He
A-5a	U-1Pd-10Zr	Solid	75%	Na
A-5b	U-2Pd-10Zr	Solid	75%	Na
B-1	U-4Pd-10Zr	Solid	55%	Na
B-2	U-4Pd-10Zr	Annular	55%	He
B-3	Materials testing for coating / liner applications			
B-4	U-10Mo	Solid	55%	Na
B-5	U-10Mo	Solid	55%	Na

Figure 37. Annular fuel casting (with copper tape grounding strap) and test matrix for AFC–3A/3B.

PUBLICATIONS:

[1]. E. Wright, et al., "Development of Advanced Ultra-High Burnup SFR Metallic Fuel Concept – Project Overview", American Nuclear Society Annual Meeting, Embedded Topical Meeting Nuclear Fuels and Structural Materials for the Next Generation Nuclear Reactors, Chicago, IL, 24-28 June 2012.

[2]. H.J. Chichester, et al., "Advanced Metallic Fuel for Ultra-High Burnup: Irradiation Tests in ATR", American Nuclear Society Annual Meeting, Embedded Topical Meeting Nuclear Fuels and Structural Materials for the Next Generation Nuclear Reactors, Chicago, IL, 24-28 June 2012.

7.4 Postirradiation Examinations of Legacy Fuels from FFTF and EBR-II

H. Chichester, D. Porter, M. Teague, INL

The baseline PIE campaign was completed on select pins from legacy FFTF oxide (12 non-destructive, 2 destructive) and metallic (8 non-destructive, 2 destructive) fuel experiments. The baseline non-destructive PIE campaign was completed on eight pins from the legacy EBR-II X496 experiment. Non-destructive PIE included visual, metrology, neutron radiography, and gamma scanning. Destructive

PIE included fission gas puncture and analysis, optical microscopy (Figure 38), micro-hardness, and chemical dissolution burnup analysis.

Examination of these legacy experiments from FFTF and EBR-II were selected based on characteristics of interest to the current FCRD Advanced Fuels Campaign, including ultra-high burnup annular MOX fuels from FFTF (ACO-3), high temperature metallic fuels clad in HT9 from FFTF (MFF-3), and very low-smear density metallic fuels from EBR-II (X496).

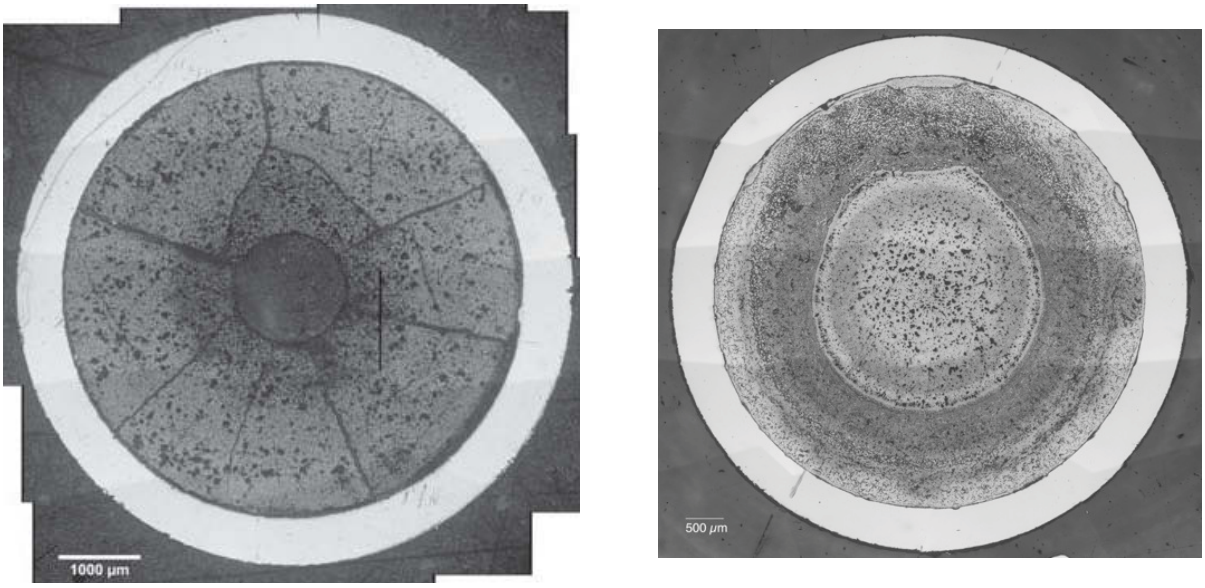

(a) (b)

Figure 38. Optical Microscopy of FFTF Fuel Experiments. (a) ACO-3 pin 150074 68.9 cm from bottom of fuel, and (b) MFF-3 pin 193045 at X/L = 0.75 from bottom of fuel

PUBLICATIONS:

[1]. M.M. Teague, Post Irradiation Examination of Legacy FFTF Oxide Fuel, June 2012, INL/LTD-12-26386.

[2]. W.J. Carmack, D.L. Porter, H.J. Chichester, S.L. Hayes, "Irradiation Performance Comparison of Experimental and Prototypic Length Metallic (U-10Zr) Fuel", 12th Information Exchange Meeting on Actinide and Fission Product Partitioning and Transmutation, Prague, Czech Republic, 24-27 September 2012.

[3]. Heather J.M. Chichester, D.L. Porter, S.L. Hayes, "Postirradiation Examination of High Burnup Metallic Fuels", HOTLAB 2012–The 49th Conference on Hot Laboratories and Remote Handling, Marcoule, France, 24-27 September 2012.

8. ANALYTIC SUPPORT

C. Unal, cu@lanl.gov, LANL

Analytic Support is focused on the analysis of the impact of novel fuel forms on reactor operations and the development of fuel fabrication models, such as sintering, casting, etc. In addition, this is the primary interface with NEAMS to identify fuels and materials data needs.

8.1 A. Metal Fuel Performance Sensitivity Assessment

8.1.1 Projected Deformation in Annular AFC-3A U-10Zr Fuel Pins & Comparison to Alternative Designs

P. Medvedev, INL

The objective of the present study was to predict the outcome of the AFC-3A annular U-10Zr fuel irradiation experiment. Specifically, the study attempted to predict whether the annular fuel will swell inward and fill the annulus, or swell outward resulting in an undesirable cladding deformation.

It was predicted that both 55% and 75% Smeared density (SD) annular fuels operating at 350 W/cm for 201 days will swell inward and partially fill the annulus which signifies a positive outcome of the experiment. Fuel and cladding geometry before and after irradiation is shown in Figure 39. The driving mechanism for such behavior is the fuel creep under the compressive stress exerted on the fuel by the cladding as a result of the fuel cladding mechanical interaction.

Comparison with the solid fuel revealed that the annular fuel is expected to swell less early in life due to the mechanical constraint provided by the cladding as shown in Figure 40. Furthermore, mechanical constraint is expected to yield a marked reduction of the axial elongation of the annular fuel as compared to the solid fuel. The prediction is based on the assumption that the annular fuel is not capable of moving axially relative to the cladding after the two come in contact. Post irradiation examination results would be very useful to assess the validity of this assumption. Specifically, the under prediction of the axial fuel growth would point to the fact that some slippage of the fuel relative to the cladding occurs after the onset of the FCMI.

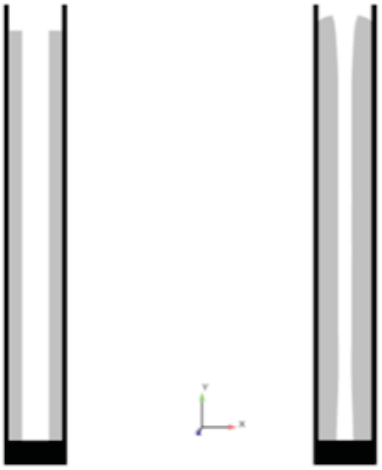

Figure 39. Results for the simulation of the annular 75% U-10Ar fuel irradiation where (a) shows fuel and cladding geometry before irradiation, (b) shows fuel and cladding geometry after irradiation.

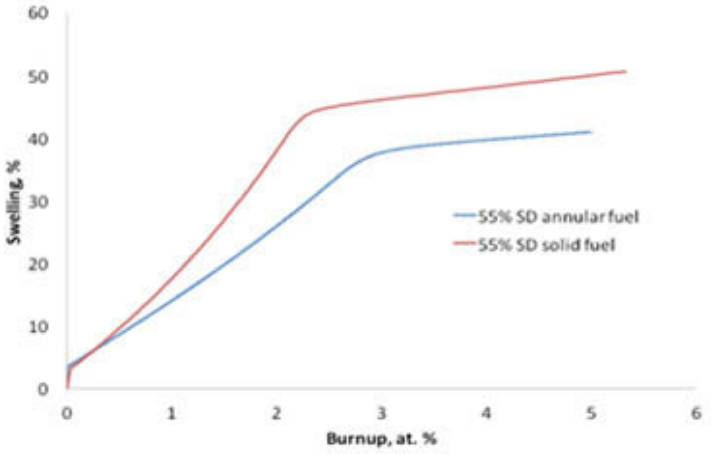

Figure 40. Swelling comparison of the solid and annular fuels, both fuels 55% smeared density (SD).

As the fuel creep plays the major role in the deformation of the annular fuel, the contributions from the thermal and irradiation induced creep to the total creep rate of fuel were examined to provide guidance for possible creep testing experiments of the fuel (separate effect tests). It was found that the irradiation induced creep dominates deformation of the fresh fuel at low temperatures. At high temperatures, and in the case of porous fuel, the thermal creep of the fuel becomes dominant and irradiation induced creep can be neglected. Fission gas induced porosity seems to accelerate fuel creep drastically. Recognizing the sensitivity of the fuel creep to the porosity, additional studies exploring this phenomenon and verifying published equations either experimentally or through computation may benefit the understanding of the annular fuel behavior.

8.1.2 Sensitivity Analysis of FEAST-Metal Fuel Performance Code

B. Williams, C. Unal, P. Edelmann, LANL

The objective of the sensitivity study was to identify important macroscopic parameters of interest to modeling and simulation of metallic fuel performance. The sensitivity study was performed using data from 6 EBR-II pins shown (red colored pins) in Table 9.

Table 9. Validation data from 6 EBR-II pins.

Data	Alloy	SUB-ID	ELM-ID
1	U-10Zr	X425	T473
2	U-10Zr	X447A	DP05
3	U-10Zr	X447A	DP11
4	U-7Pu-8Zr	X425	T452
5	U-7Pu-8Zr	X425A	T456
6	U-19Pu-10Zr	X430B	T654
7	U-19Pu-6Zr	X441A	DP24
8	U-19Pu-10Zr	X441A	DP45
9	U-19Pu-10Zr	X441A	DP21
10	U-19Pu-14Zr	X441A	DP29
11	U-22Pu-10Zr	X430B	T670
12	U-26Pu-10Zr	X430B	T684

Sensitivity ranking methodology was deployed to narrow down the selected parameters for the current study. There are approximately 84 calibration parameters in the FEAST-Metal code, of which 32 were ultimately used in Phase II of this study.

The fuel thermal conductivity and gas release models were most influential in terms of explaining overall output variability, and are therefore targets for additional calibration to further constrain their parameters. We considered all results to recommend a ranking of models that can be considered for further improvements. Our model ranking is as follows:

- Fission gas release and swelling,
- Fuel and clad conductivity,
- Species diffusion, and
- Fuel creep.

We identified eighth modeling parameters used in the FEAST code having a significant impact on key performance outputs as shown in Table 10.

Table 10. Recommended Modeling Parameters. Eight most important ones with high confidence are in read type; 13 bleed colored parameters should be kept in the list until confidence to eliminate or keep them is increased with further studies.

Gas Release Model	
gacten	Gas activation energy for diffusion
rb1	Radius of bubble – 1
rb2	Radius of bubble – 2
trprob	Transition probability bubble – i to bubble– i = 1 (collision)
kb1nuc	Bubble – 1 nucleation constant
egb1	Empirical bias factor for gas diffusion to closed bubble – 1
dgo	Gas diffusion factor
ebb2	Empirical bias factor, diffusion to closed bubbles
ebb3	Empirical bias factor, diffusion to open bubbles
Species Diffusion Model	
qduzr	Heat of transport for U-Zr delta phase
eht2	Effective heat of transport 2 (U-Pu-Zr, delta)
doduzr	Diffusion coefficient for U-Zr delta phase
doauzrpu	Multiplier for Diffusion coefficients for U-Pu-Zr alpha – delta – beta phases
Fuel Creep Model	
qbuzrpu	Creep Enhancement to Model Yield Stress enhp (2)
es3	Creep Enhancement to Nodel Yield Stress enhp (3)
Thermal Properties	
fkb	Fuel thermal conductivity coefficient b
skfpc	Sodium infiltration coefficient
kclas	Thermal conductivity HT9
fkc	Fuel thermal conductivity coefficient c
Others	
ennn	Dislocation Creep Constant (nnn)
fse	Free surface energy

8.1.3 A Species Distribution Kernel implemented into the 3D BISON Framework for the Analysis of Metallic Fuels

W. Zhou, N. Carlson, C. Unal, LANL

The typical metallic fuel performance problem concerns the thermal/mechanical behavior and constituent redistribution in U-Pu-Zr metallic nuclear fuel. Thermal distribution and constituent redistribution depend strongly upon each other and are therefore fully coupled in sodium cooled fast reactor applications in this work. Mechanical behavior is not modeled yet. Substantial U and Zr redistribution has been observed in irradiated fuel, which is subjected to intense radial thermal gradients. This change in local composition affects the mechanical and thermal properties of the fuel as well as the radial power distribution. The modeling and simulation of constituent migration is therefore an essential component of the simulation of fuel performance. A 3-D model was developed and a 3-D benchmark test problem based on a U-Pu-Zr fuel design for the conceptual 4S reactor was defined and implemented in the MOOSE/BISON code, which is a high-performance framework for fully coupled multi-physics problems.

The solution kernels of BISON for the thermal transport and mechanical behavior are reasonably well developed and they are used without modifications in this work. Instead we concentrate on the

development/modification of the solution kernel for diffusion of uranium and zirconium in the metallic fuel.

The continuity equation for zirconium can be expressed as follows:

$$\frac{\partial C_{Zr}}{\partial t} = -\nabla \cdot \vec{J}_{Zr} + s$$

Where:

C_{Zr}: Zirconium concentration (mol/m^3),

J_{Zr}: Interdiffusion flux (atom/m^2/s),

s: Zirconium production rate by fission. The Zirconium yield is 0.2 for the fission of Plutonium.

Within a single γ phase field the zirconium interdiffusion flux is given by

$$J_{Zr} = -D_{Zr}^{eff}\left(\nabla C_{Zr} + \frac{Q_{Zr} C_{Zr}}{RT^2}\nabla T\right)$$

Where:

D_{Zr}^{eff}: Effective interdiffusion coefficient of zirconium in γ phase (m^2/s),

Q_{Zr}: Heat of transport of zirconium in γ phase (J/mol),

R: Gas constant (8.314 J/mol/K),

T: Local fuel temperature (K).

Within a dual phase field such as $\alpha+\delta$ and $\beta+\gamma$, the driving force for diffusion is affected by the solubility of zirconium in the precipitation phases.

$$J_{Zr} = -V_1 D_{Zr,1}^{eff} C_{Zr,1}\frac{\Delta\bar{H}_{s,1} + Q_{Zr,1}}{RT^2}\nabla T - V_2 D_{Zr,2}^{eff} C_{Zr,2}\frac{\Delta\bar{H}_{s,2} + Q_{Zr,2}}{RT^2}\nabla T$$

Where:

V_1: Volume fraction of a phase-1

Note that subscript "1" represents the first phase and subscript "2" represents the second phase.

The above formulation as given in FEAST code did not produce good results. We made some modification to the formulation of the flux in the two-phase region. We made the assumption that a local equilibrium between two phases is maintained at each point in a temperature gradient through instantaneous adjustment of the phase fractions via rapid local diffusion processes. This means that C_{Zr} is constrained to lie on the solubility curve, which we will denote by $C_{Zr,\alpha}(T)$, and as a consequence $\nabla C_{Zr} = C_{Zr,\alpha}\nabla T$. The general flux in the 2-phase region is then defined to be the phase fraction weighted linear combination of the above two equations:

$$J = -V_\alpha D_\alpha\left(C'_{Zr,\alpha}(T) + C_{Zr,\alpha}(T)\frac{Q_{Zr,\alpha}}{RT^2}\right)\nabla T - V_\beta D_\beta\left(C'_{Zr,\beta}(T) + C_{Zr,\beta}(T)\frac{Q_{Zr,\beta}}{RT^2}\right)\nabla T$$

where $V_\alpha + V_\beta = 1$ and $V_\alpha(C_{Zr}, T)$ is the phase fraction of α at temperature T and average composition C_{Zr} and is defined by the lever rule.

The other primary modification is to add some artificial diffusion to the 2-phase flux. In a $\alpha + \beta$ region (here α and β are any two generic phases), we add $-(V_\alpha D_\alpha \lambda_\alpha + V_\beta D_\beta \lambda_\beta)\nabla C_{Zr}$ to the flux, where V_α and V_β are molar fractions, D_α and D_β are diffusion coefficients, and λ_α and λ_α are numerical artificial diffusion coefficients. The amount of artificial diffusion that needs to be added to avoid spurious oscillations depends on the strength of the Soret advection term and the mesh spacing. This is roughly equivalent to a simple upwinding advection scheme, at least in 1D. In order to minimize the amount of artificial diffusion needed, as well as decently approximate the solution discontinuities that will develop in the domain, a fine mesh is required in the radial direction. We consider a benchmark problem given on the left side of Figure 41.

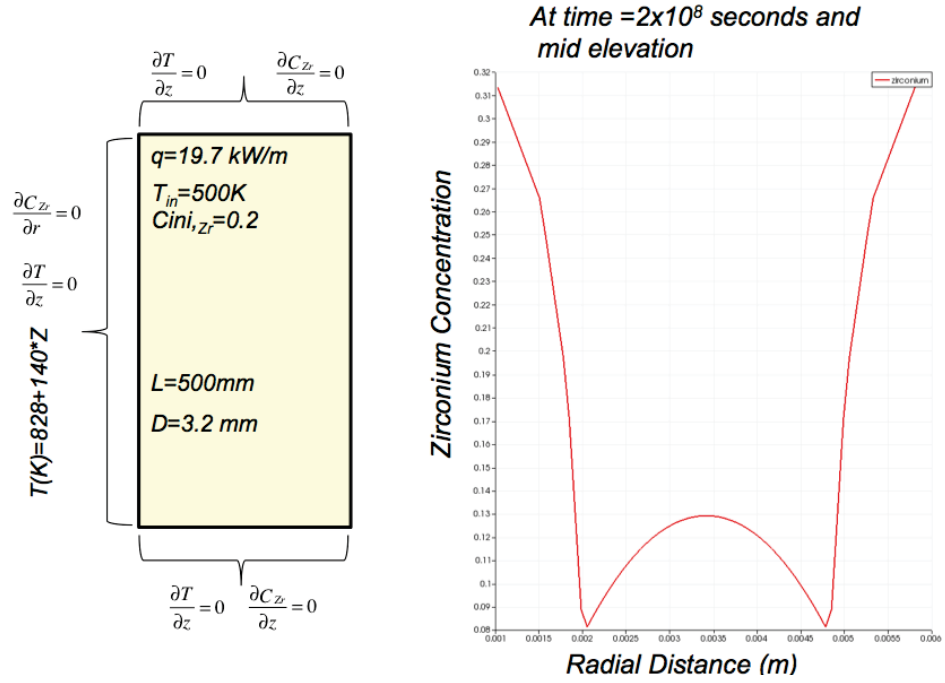

Figure 41. Diffusion benchmark problem and radial zirconium concentration at the mid elevation at $2x10^8$ seconds.

The solution used a variable time step scheme and artificial diffusion coefficients of 0.2. The radial zirconium profile at time 2 × 108 seconds shows a depleted zirconium region in the mid section of the fuel rod as we observe in experiments. The verification and validation of the diffusion kernel is underway.

8.2 Casting Modeling and Simulation

J. Crapps, J. Galloway, D. DeCroix, C. Unal, LANL

8.2.1 Argon Gas in the Mold

Prior modeling and simulation work on this project was performed using the Truchas code for evacuated molds. In these cases, the casting and mold filling is simplified in the sense that the molten metal freely flows into the mold. However, because the metal fuel being considered contains americium, a cover gas is necessary to keep the americium in solution while the metal cools and solidifies. Americium has a low vapor pressure, and when the molten metal flows into an evacuated mold, the gaseous americium evolves out of the molten metal. Therefore, argon gas is being used to fill the mold prior to the

molten metal flowing into the mold. Because there is another fluid (gas) in the mold, the molten metal must displace the gas and there in lays another problem to overcome. We are using a two-fluid CFD method to simulate both the argon and molten metal and their fluid dynamic interactions during the mold fill process. Because of the argon, the molten metal "bubbles" into the mold increasing the time to fill, compared to an evacuated mold. The argon gas can get trapped and surrounded by the molten metal, which can cause breaks in the cast fuel rods. The presence of the argon, which is necessary to keep the americium in solution, greatly affects the fluid flow mechanics and mold fill processes (see Figure 42).

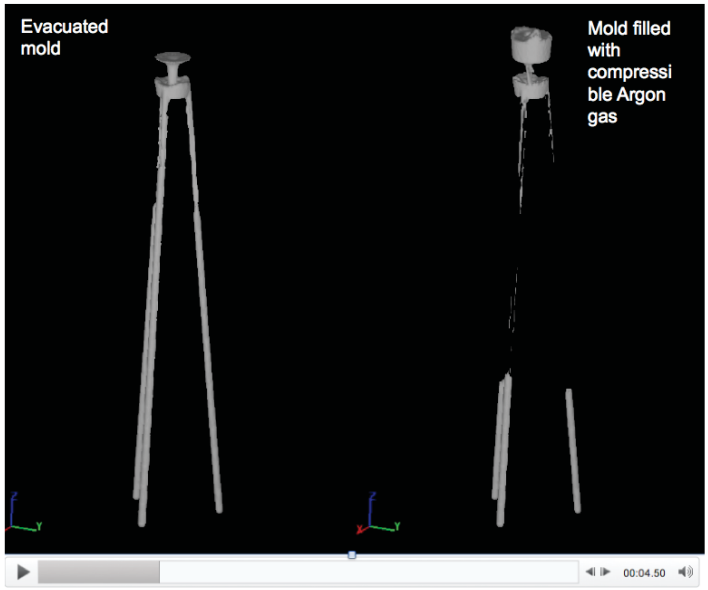

Figure 42. A snapshot of casting with and without argon at 4.5 seconds.

8.2.2 Proper Venting

Due to the presence of argon in the mold prior to filling, various venting scenarios have been simulated. Essentially the mold must now include one or more vents to allow the argon to escape as the molten metal displaces it in the mold. Without vents, the argon must flow back out the top of the mold and crucible to escape and not get trapped inside the mold. We have begun to investigate where to place vents and how many are necessary to minimize the possibility of argon bubbles getting trapped and causing a break in the cast fuel rods. We recognize there will be physical and mechanical challenges to actually put vents in the mold and test at the BSC. The modeling and simulation results will be used to evaluate possible venting methods while working closely with colleagues performing the experimental work. Initial simulation results show a dramatic reduction in the void fraction (trapped argon gas) in the cast fuel rods (see Figure 43).

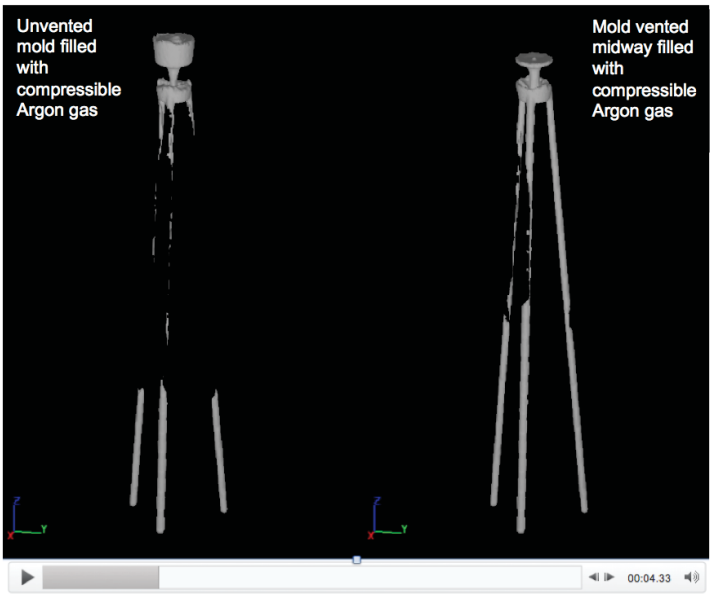

Figure 43. A snapshot of casting with and without vent in an evacuated mold at 3.2 seconds.

8.2.3 Physical Properties of the Molten Metal

Two studies were performed to investigate flow parameters at extreme values and then at values 20% above and below the nominal values. In our study of the effects of various physical parameters, such as wetting angle, surface tension, viscosity, etc., one of the metrics we used to identify a "sensitive" parameter was the void fraction in the casting. We calculate the total metal volume in the cast rod and subtract it from the mold volume to calculate the void fraction. We were attempting to determine which material properties were the most sensitive (or helpful) in minimizing the void fraction. This was used to provide guidance to the experimental team as to which liquid metal properties they needed to measure. We have show qualitative agreement between simulations and rod cast from the BSC. A two level factorial design of experiments considering three design variables was employed in each case. We performed a design of experiments study to quantify several material properties and their impact on effective mold fill, for both circular and annular fuel rod geometries. The most important fuel material property to be measured is the wetting angle of the molten metal on the coated mold material (coated graphite). The second most important property to measure is the surface tension of the molten metal in argon gas at the design mold pressure. The magnitude of these material properties had the largest effect on whether the mold casting processes produced large voids in the fuel rods.

The nominal mold fill method used in the above study was the gravity assisted top-fill method of the Idaho National Laboratory Bench Scale Casting facility. Alternative mold fill methods were investigated and using a bottom-fill method shows promise. In the bottom-fill method, the molten metal is injected into the bottom of the mold and the argon cover gas is allowed to escape through vents at the top of the mold. This allows for a smooth, uniform fill of the mold, where as the top-fill geometry has a counter-flow condition of the molten metal and argon cover gas. The mold is initially filled with argon, and using a top fill method, the molten metal must flow downward into the mold and the argon is displaced by the metal and must flow upward out of the mold. This counter-flow condition creates large voids in the cast because bubbles of argon get trapped as the metal flows into the mold. We also investigated various venting schemes for the top fill casting process and this also shows some promise to mitigate the void formation.

8.3 Modeling of Volatile Species Retention Experiments

N. Carlson, C. Unal, LANL

Metallic nuclear fuel is a candidate transmutation fuel form for advanced fuel cycles. Americium is likely to be a minor constituent of the fuel, but concerns have been raised about the possible excessive loss of americium during casting through volatility because of its high vapor pressure. A number of experiments have been done using americium and other volatile surrogate metals, like manganese and samarium that are easier to work with, in order to assess the potential volatility losses. The present task was to model and simulate the volatile species loss experiments.

Figure 44 shows a schematic for the model. The experimental system is divided into four components: the liquid metal alloy melt pool at the bottom of the crucible (**M**), the gas above the melt within the crucible (**A**), the gas outside the crucible contained within the furnace (**B**), and the inside surface of the crucible lid (**C**) where condensation of the volatile species is allowed to occur (the cold trap). The latter component is motivated by experimentally observed condensation on the crucible lid.

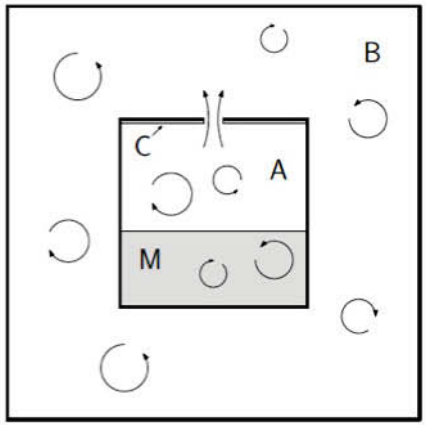

Figure 44. Schematic of the system level model.

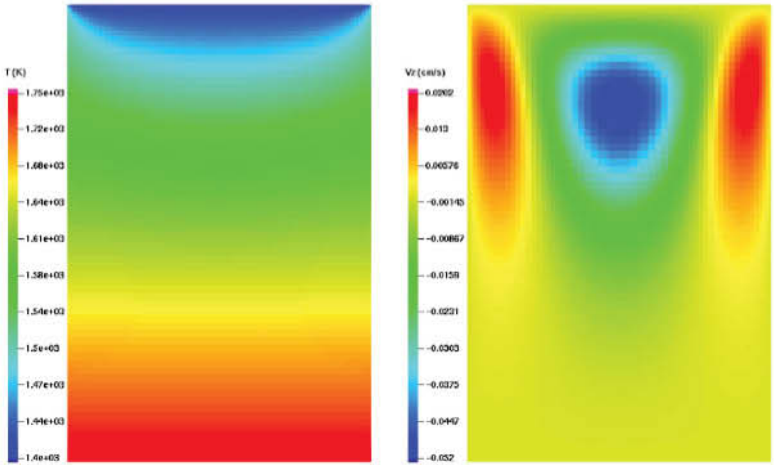

Figure 45. Steady-state profiles for temperature (left) and vertical velocity (right) over a vertical cross section through the axis of the cylindrical domain. Temperature ranges from 1750 K along the bottom, decreasing linearly up the sides to 1500 K at the top, and approximately 1400 K along the top. Maximum vertical velocity is approximately 0.5 mm/s.

A collection of three-dimensional, 'full-physics' simulations of the relevant governing PDEs were performed to answer several questions.

- *Buoyancy-driven convection in the crucible cavity; volatile transport.* The steady state results, attained after ~5 minutes starting from a stagnant gas, are shown in Figure 45. The temperature and vertical velocity profiles are plotted on a vertical cross section through the domain axis. What is immediately clear from the results is that there is very little convection within this small confined region. Unless there is another source driving flow in the gas, the conclusion is that heat and mass transport in the crucible gas will be dominated by diffusion. Indeed the temperature reaches its steady state profile within several seconds.
- *Buoyancy-driven flow in the furnace with uncovered crucible.* The final set of simulations considered buoyancy-driven convection of the cover gas in the GACS furnace with an uncovered crucible. Only the gas-filled region was modeled, not the furnace walls nor the crucible or metal melt in the bottom of the crucible. The crucible was uncovered so that the gas-filled region extends into the crucible, see Figure 46.

Figure 46 and Figure 47 show the temperature and vertical velocity after the flow has settled in an approximate steady flow pattern. As expected a hot plume rises from the crucible and the flow sinks along the furnace wall. The maximum velocity is approximately 160 cm/s. However, the more significant observation can be seen in the flow detail from Figure 47. The rising plume past the crucible produces a recirculating flow zone in the mouth of the open crucible. The flow is fairly strong with a peak inflow velocity of about 20 cm/s at the opening. This suggests that with the present crucible geometry, convective transport of a volatile species within the crucible cannot be ignored and can be the dominant loss process, carrying the volatile into the outer furnace.

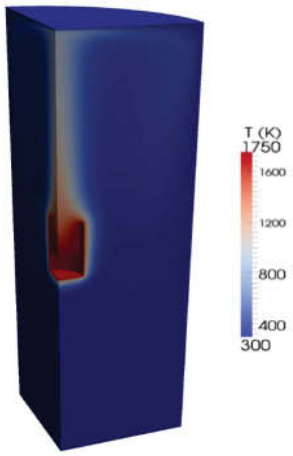

Figure 46. Buoyancy-driven gas convection (30 kPa Ar) in GACS furnace enclosure with open crucible (quarter symmetry). Plot of temperature after the flow pattern has become nearly steady. Temperature fixed at 300 K at the furnace boundary and 1750 K at the crucible/melt boundary.

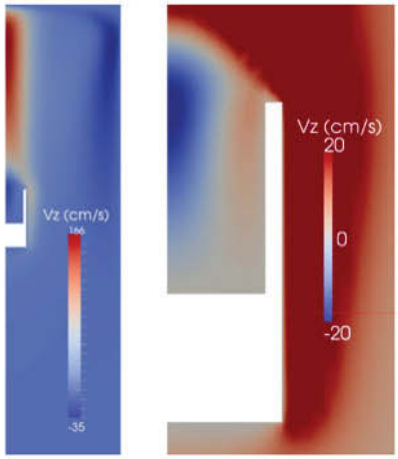

Figure 47. Vertical gas velocity over a vertical cross section through axis of the furnace enclosure (left) and close-up detail near the crucible (right). Maximum velocity is approximately 1.7 m/s. The detail plot shows a recirculating flow into the crucible with a maximum velocity of about 20 cm/s into the crucible.

Two additional basic scenarios were modeled. In the first, the crucible was covered with a vented lid to correspond to the experiments. In the second, the crucible was uncovered and opened to the furnace enclosure.

- *Covered Crucible.* Simulations show that saturation of the cover gas inside the crucible with Am occurs very rapidly through diffusion alone. Buoyancy-driven convection is insignificant, even with large thermal gradients, due to the small size of the crucible cavity.
- *Uncovered Crucible.* Simulations (and common sense) suggest there is strong buoyancy-driven flow in the furnace cover gas due to the large temperature difference between the furnace wall and crucible. As a consequence, any Am that escapes the crucible will quickly mix and be available to condense on the cool furnace wall. The losses could be controlled by adjusting the crucible height.

8.4 Master Sintering Curve (MSC) – Densification Based Finite Element (DFEM) Model for the Sintering of Ceramic Nuclear Fuels.

C. Unal, LANL

Oxide nuclear fuel pellets are cold pressed and sintered from a powder feedstock. For a given powder feedstock, we demonstrate that it is possible to predict together the densification and shrinkage during the sintering process for an arbitrary thermal history. The MSC-DFEM framework assumes that sintering is dominated by a single diffusion mechanism and the corresponding activation energy is the only adjustable

parameter in our approach and represents a characteristic of the powder stock. We conclude that the MSC-DFEM approach can be used to optimize the sintering process, because changing the properties of the powder by using a modified processing protocol can modify the activation energy,

The MSC-DFEM approach has three major components: a) develop the Master Sintering Curve (MSC) model characteristic to the particular powder stock, ii) perform densification-based finite-element (DFEM) simulations using the MSC as input to calculate the material response under deformation, and iii) use a Vision system to characterize the geometry of the pellet in the green and sintered states. The later is used to compare with the results of our numerical simulations and will ultimately be used to validate our MSC-DFEM approach.

We demonstrated the viability of the MSC-DFEM framework to capture the densification and size changes of the pellet during sintering (see Figure 48). In particular our model predicts the correct size of the hour-glass shape of the sintered pellet observed experimentally. We demonstrate that the MSC-DFEM model predicts the correct shrinkage even for pellets sintered with a different initial geometry and following a different thermal path. At this time our model does not capture the asymmetric aspect of the hour-glassing in the sintered pellet. Potential limitations of our model are linked to the presence of asymmetrical frictional forces in the die during compaction and the asymmetrical nature of powder packing. Also, sintering usually occurs on a non-shrinking setter. None of these effects is taken into account explicitly in the present incarnation of our model. A systematic experimental and modeling effort will be pursued to improve the MSC-DFEM model.

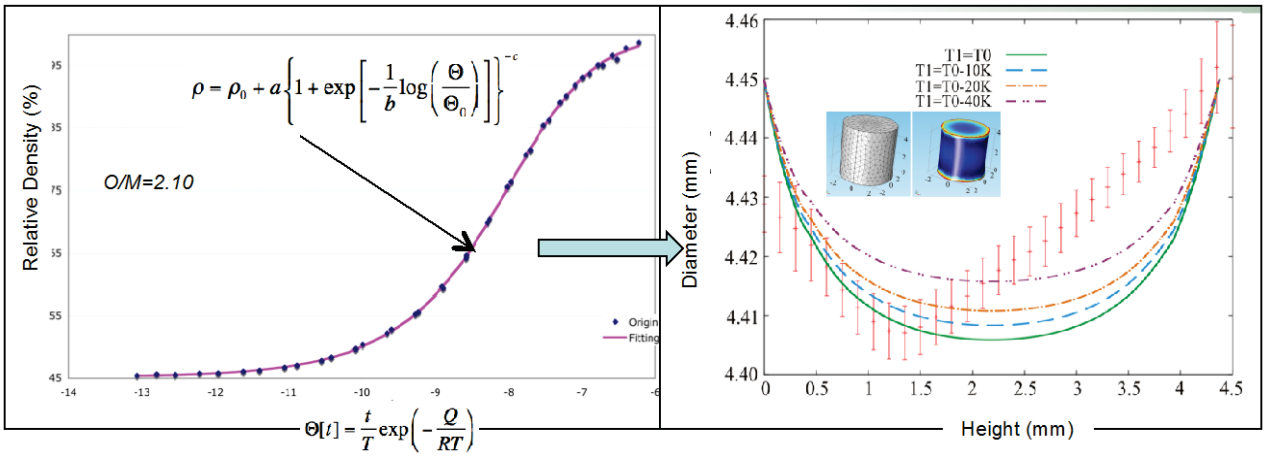

Figure 48. Master sintering curve for uranium oxide powder obtained from AREVA (left) and prediction of geometry of a pellet using MSC-DFEM method.

8.5 Advanced Fuels Impact on LWR Operations

M. Todosow, N. Brown, G. Raitses, H. Ludewig, A. Aronson, BNL

Nodal core simulators provide a state-of-the-art tool to assess the full-core neutronic performance and safety characteristics of novel nuclear reactor fuel concepts. In order to have the requisite confidence for performing these analyses for a typical pressurized-water reactor (PWR), BNL has developed a three-dimensional core model for the PARCS core simulator for a reactor based on a Westinghouse AP1000. Cross-sections have been generated with the BOXER and TRITON multigroup lattice physics codes, and the SERPENT Monte Carlo code (Figure 49). These codes were benchmarked at the lattice level and then independently utilized to generate three distinct PARCS models at beginning-of-life, equilibrium conditions.

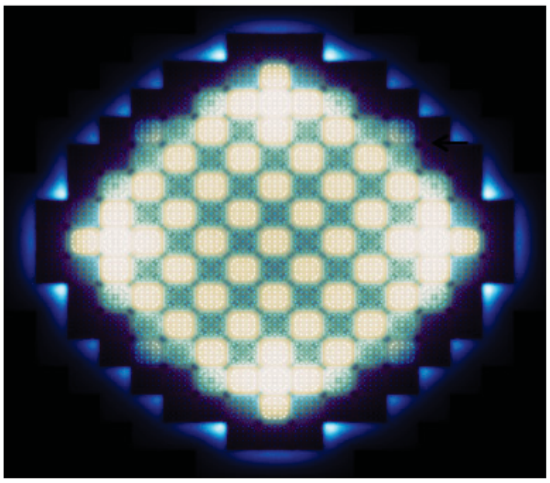

Figure 49. SERPENT Model for AP1000 Core.

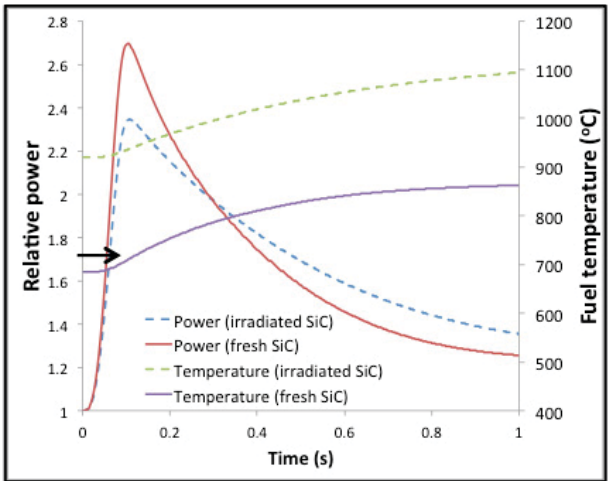

Figure 50. Results of PARCS Simulation of RIA with FCM Fuel.

Key core characteristics were compared for the three models and relative to the data in the AP1000 FSAR. The models show reasonable agreement thereby "validating" the model to serve as a testing platform for the ongoing evaluations of novel nuclear fuel concepts that may exhibit enhanced accident tolerance; the present effort is focused on fully ceramic microencapsulated (FCM) fuel as discussed below.

A PARCS full-core model of a "representative" PWR based on the AP1000 was also developed for a core fully loaded with FCM fuel. These analyses were performed to evaluate the response to a reactivity insertion accident (RIA) in a commercial PWR with FCM fuel to address the issues of the significantly higher power density, and transients that occur on significantly shorter time-scales in a PWR than in the HTGR for which the fuel has been designed and qualified. SERPENT has been selected as the tool for cross section generation due to the ability of SERPENT to explicitly model the FCM fuel geometry as well as the ability of a modified version of SerpentXS to perturb only the fuel kernel temperatures for off-reference branch cases. In order to increase the fidelity of the simulation, the parameters for the fuel and matrix material in the PARCS thermal-hydraulic module were modified to reflect the different geometry and materials. Data for both un-irradiated and irradiated SiC were obtained from the literature and included in the analyses. Improved data have been requested from Oak Ridge National Laboratory (ORNL) but have not been available for inclusion in the present analyses; a revision to the present report is planned when these data are received. An example of the initial results from this study is shown in Figure 50. The details of the study are documented in the following report, which satisfied Milestone M3FT-12BN0202012: N. Brown, et al, Neutronic Evaluations of a PWR with Fully-Ceramic-Micro-Encapsulated (FCM) Fuel/year-end summary report, FCRD-FUEL-2012-000379, Sept. 30, 2012.